Electroweak Supersymmetry (EWSUSY) in the NMSSM

Taoli Cheng[1] and Tianjun Li[1, 2, 3]

[1]*State Key Laboratory of Theoretical Physics, Institute of Theoretical Physics, Chinese Academy of Sciences, Beijing 100190, P. R. China*

[2]*School of Physical Electronics, University of Electronic Science and Technology of China, Chengdu 610054, P. R. China*

[3]*George P. and Cynthia W. Mitchell Institute for Fundamental Physics and Astronomy, Texas A&M University, College Station, TX 77843, USA*

Abstract

To explain all the available experimental results, we have proposed the Electroweak Supersymmetry (EWSUSY) previously, where the squarks and/or gluino are heavy around a few TeVs while the sleptons, sneutrinos, Bino, Winos, and/or Higgsinos are light within one TeV. In the Next to Minimal Supersymmetric Standard Model (NMSSM), we perform the systematic χ^2 analyses on parameter space scan for three EWSUSY scenarios: (I) R-parity conservation and one dark matter candidate; (II) R-parity conservation and multi-component dark matter; (III) R-parity violation. We obtain the minimal χ^2/(degree of freedom) of 10.2/15, 9.6/14, and 9.2/14 respectively for Scenarios I, II, and III. Considering the constraints from the LHC neutralino/chargino and slepton searches, we find that the majority of viable parameter space prefered by the muon anomalous magnetic moment has been excluded except for the parameter space with moderate to large $\tan\beta$ ($\gtrsim 8$). Especially, *the most favorable parameter space has relatively large* $\tan\beta$*, moderate* λ*, small* $\mu_{\rm eff}$*, heavy squarks/gluino, and the second lightest CP-even neutral Higgs boson with mass around 125 GeV.* In addition, if the left-handed smuon is nearly degenerate with or heavier than Wino, there is no definite bound on Wino mass. Otherwise, the Wino with mass up to ~ 450 GeV has been excluded. Furthermore, we present several benchmark points for Scenarios I and II, and briefly discuss the prospects of the EWSUSY searches at the 14 TeV LHC and ILC.

PACS numbers: 12.60.Fr, 14.80.Da, 14.80.Ly

I. INTRODUCTION

Supersymmetry (SUSY) is the most promising new physics beyond the Standard Model (SM). From the theoretical point of view, it solves the gauge hierarchy problem in the SM, and is consistent with the Grand Unified Theories (GUTs) due to the gauge coupling unification in the supersymmetric SMs (SSMs). From the phenomenological point of view, the electroweak (EW) gauge symmetry can be broken radiatively due to the large top quark Yukawa coupling, and the lightest supersymmetric particle (LSP) such as neutralino can be a cold dark matter canidiate if R-parity is conserved. Also, in the Minimal SSM (MSSM), the lightest CP-even neutral Higgs boson is predicted to be lighter than about 130 GeV (For a review, see Ref. [1].), which is compatible with the Higgs boson with mass around 125 GeV discovered by the ATLAS and CMS Collaborations in July 2012 [2, 3].

Inspired by the LHC Higgs [4] and SUSY [5] searches, the experimental results/constraints on B physics [6, 7] and Flavour Changing Neutral Current (FCNC) [8–10], anomalous magnetic momentum of the muon [11], dark matter relic density from WMAP experiment [12], and direct dark matter search from XENON100 experiment [13], we proposed the Electroweak Supersymmetry (EWSUSY): the squarks and/or gluino are heavy around a few TeVs while the sleptons, sneutrinos, Bino, Winos, and/or Higgsinos are light within one TeV [14]. To realize the EWSUSY in the MSSM, we considered the non-universal gaugino masses, universal/non-universal scalar masses, and universal/non-universal trilinear soft terms, inspired by the Generalized Minimal Supergravity (GmSUGRA) [15, 16]. For the later and relevant studies, see Refs. [17–25]. Moreover, the heavy squarks are prefered by the SUSY FCNC and CP violation problems. And the light electroweak SUSY sector is very promising on both model building and phenomenological study.

Let us briefly review the current LHC Higgs, SUSY and B physics searches and the anomalous magnetic momentum of the muon in the SSMs. The ALTAS and CMS Collaborations have released their latest results for the Higgs boson searches by various channels [4], which indicate a highly SM-like Higgs particle with mass around 125 GeV. The concrete experimental results will be given in Section III. However, the SUSY searches at the LHC still suffer from the null results [5]. Until now, the first two generation squarks with mass less than around 1.5 TeV have been excluded in the Contrainted MSSM (CMSSM) or Minimal Supergravity (mSUGRA). For the simple decay chains ($\tilde{g} \to t\bar{t}\tilde{\chi}_1^0$ or $\tilde{g} \to b\bar{b}\tilde{\chi}_1^0$) in the sim-

plified models where all the supersymmetric particles (sparticles) except the LSP neutralino χ_1^0 and gluino are decoupled, gluino with mass below about 1.3 TeV has been excluded for the LSP lighter than $\sim$ 500 GeV. With the LSP below 300 GeV, the masses of light stop and sbottom have been pushed up to $\sim 600 - 700$ GeV in different decay modes except for the mass-degenerate region. Moreover, the first evidence of rare decay $B_s^0 \to \mu^+\mu^-$ has been found by the LHCb Collaboration recently [6]. The value of branching fraction $3.2^{+1.5}_{-1.2} \times 10^{-9}$ leaves very small room for the contributions from new physics like SUSY beyond the SM.

Interestingly, the 3.6σ deviation of the anomalous magnetic moment of the muon $(g_\mu - 2)/2$: $\Delta a_\mu = a_\mu^{\rm exp} - a_\mu^{\rm SM} = (2.87 \pm 0.8) \times 10^{-9}$ [11] may imply the new physics beyond the SM around the electroweak scale. In the SSMs, the light smuon, muon-sneutrino, Bino, Winos, and Higgsinos would contribute to Δa_μ [26–30]. The SUSY contributions could roughly be approximated as $\sim 1.3 \times 10^{-9} {\rm sgn}(\mu M_2) \left(\frac{100{\rm GeV}}{M_{\rm SUSY}}\right)^2 \tan\beta$, where $M_{\rm SUSY}$ denotes the typical mass scale of relevant sparticles. With $M_{\rm SUSY} \sim$ several hundred GeV and $\tan\beta \sim \mathcal{O}(10)$, the discrepancy can be explained. However, to obtain the Higgs boson mass 125 GeV in the CMSSM/mSUGRA, we require relatively large gaugino mass $M_{1/2}$ and/or scalar mass M_0, which correlate the squark and slepton masses. Thus, it is very difficut to obtain the above Δa_μ in the CMSSM/mSUGRA. Of course, the above Δa_μ can be realized in the MSSM with the EWSUSY due to the non-universal gaugino masses, scalar masses, as well as trlinear soft terms [14].

The simplest extension of the MSSM is the Next-to-MSSM (NMSSM), where a SM singlet Higgs field S is introduced (For a review, see Ref. [31].). In the NMSSM, we can solve the μ problem dynamically while keep the above attractive features in the MSSM. In fact, there exists some degree of fine-tuning to have the Higgs boson mass about 125 GeV in the MSSM. Interestingly, we can lift the SM-like Higgs boson mass and then solve such fine-tunging problem in the NMSSM for two reasons: (1) the F-term contribution to the tree-level Higgs potential from superpotential term $\lambda S H_d H_u$, where H_d and H_u are one pair of Higgs doublets in the SSMs. This contribution to the Higgs mass square is proportional to $\lambda^2 \sin^2 2\beta$, where $\tan\beta$ is the ratio of the Vacuum Expectation Values (VEVs) of H_u and H_d; (2) The pushing up effect from the diagonalization of Higgs boson mass matrix since the second lightest CP-even neutral Higgs boson can be SM-like. If the Higgs boson decay branching fractions were indeed deviated from the SM predictions, such devivations may be explained in the NMSSM as well. Thus, the NMSSM has been studied extensively after the

Higgs boson discovery [32–40]. To obtain the SM-like Higgs boson mass around 125 GeV in the previous studies of the constrained NMSSM, one usually considered the small $\tan\beta$ ($\tan\beta \leq 4$) and large λ ($\lambda \sim 0.6 - 0.7$) regime, which gives relatively large tree-level F-term contribution. However, the SUSY contributions to the anomalous magnetic moment of the muon Δa_μ are generically smaller than about 4.0×10^{-10} [33, 38].

In this paper, with the GmSUGRA for supersymmtry breaking soft terms, we consider the following three EWSUSY scenarios in the NMSSM: (I) R-Parity Conservation (RPC), and the LSP neutralino is the only dark matter candidate; (II) R-parity conservation and multi-component dark matter. So the LSP neutralino relic density just needs to be smaller than the observed dark matter density; (III) R-Parity Violation (RPV). So the LSP can be the lightest neutralino, light stau, or tau sneutrino, which will decay into the SM particles through RPV superpotential terms. In the parameter space scan, we consider the experimental results from the LHC Higgs seaches, B physics, Δa_μ, and dark matter relic density, etc. The Degree Of Freedom (DOF) from the experimental data is 15, 14, and 14 respectively for Scenarios I, II, and III. We perform the detailed χ^2 analyses, and find that the minimal χ^2/DOF are 10.2/15, 9.6/14, and 9.2/14 respectively for Scenarios I, II, and III. Similar to the previous studies, we still obtain some viable parameter space where the light stop and gluino are light within 1 TeV for small $\tan\beta \leq 4$ and large $\lambda \sim 0.6 - 0.7$. Employing the constraints from the LHC neutralino/chargino and slepton searches, we show that the majority of viable parameter space prefered by Δa_μ has been excluded except for the parameter space with moderate to large $\tan\beta$ ($\gtrsim 8$). In particular, *in the most favorable parameter space, we have relatively large* $\tan\beta$*, moderate* λ*, small* $\mu_{\rm eff}$*, heavy squarks/gluino, and the second lightest CP-even neutral Higgs boson being SM-like.* The SM-like Higgs boson mass is lifted by the radiative corrections due to the large stop masses and pushing up effect [35]. In addition, if the left-handed smuon is nearly degenerate with or heavier than Wino, there is no definite bound on Wino mass, which can be as light as 230 GeV. While if the left-handed smuon is lighter than Wino, the Wino with mass below ~ 450 GeV has been excluded. Furthermore, we present a few benchmark points for Scenarios I and II where χ^2/DOF can be around one, and we briefly discuss the prospects of the EWSUSY searches at the $\sqrt{s} = 14$ TeV LHC (LHC-14) and ILC (e^+e^- linear collider with designed center mass energy of 500 GeV – 1 TeV).

This paper is organized as follows. In Section II, we give a brief review of the EWSUSY

from the GmSUGRA and the supersymmetric contributions to the anomalous magnetic moment of the muon. In Section III, the numerical results employing χ^2 statistic test are given. And we present the systematic analyses of the resulting distribution of viable parameter space and sparticle spectra. In Section IV, the LHC neutralino/chargino and slepton search constraints are considered, and the future searches of the electroweak SUSY sector are discussed. We also present some benchmark points. Finally in Section V, we summarize our work briefly.

II. A BRIEF REVIEW OF THE EWSUSY AND $(g_\mu - 2)/2$

In this Section, we will briefly review the EWSUSY from the GmSUGRA as well as the SUSY contributions to the anomalous magnetic moment of the muon.

A. The EWSUSY from the GmSUGRA in the NMSSM

The EWSUSY, which can be realized in the GmSUGRA [15], has a mass hierarchy for the colored and uncolored sparticles: squarks and/or gluino are heavy around several TeV while the sleptons, sneutrinos, Bino, Winos, and/or Higgsinos are light within one TeV [14]. In the GmSUGRA, the gauge coupling relation and gaugino mass relation at the GUT scale are

$$\frac{1}{\alpha_2} - \frac{1}{\alpha_3} = k \left(\frac{1}{\alpha_1} - \frac{1}{\alpha_3} \right) , \tag{1}$$

$$\frac{M_2}{\alpha_2} - \frac{M_3}{\alpha_3} = k \left(\frac{M_1}{\alpha_1} - \frac{M_3}{\alpha_3} \right) , \tag{2}$$

where k is the index and equal to 5/3 in the simple GmSUGRA. Assuming a univeral gauge coupling at the GUT scale ($\alpha_1 = \alpha_2 = \alpha_3$) for simplicity, we obtain a simple gaugino mass relation

$$M_2 - M_3 = \frac{5}{3} \left(M_1 - M_3 \right) . \tag{3}$$

The univeral gaugino mass relation in the mSUGRA $M_1 = M_2 = M_3$ is just a special case of this general one. Choosing M_1 and M_2 to be free input parameters which vary around several hundred GeV for the EWSUSY, we get

$$M_3 = \frac{5}{2} M_1 - \frac{3}{2} M_2 , \tag{4}$$

which could be as large as several TeV or as small as several hundred GeV, depending on specific values of M_1 and M_2.

The general supersymmetry breaking scalar masses at the GUT scale are given in Ref. [16]. Taking the slepton masses to be free, we obtain the following squark masses

$$M^2_{\tilde{Q}_i} = \frac{5}{6}(M_0^U)^2 + \frac{1}{6}M^2_{\tilde{E}_i^c} , \tag{5}$$

$$M^2_{\tilde{U}_i^c} = \frac{5}{3}(M_0^U)^2 - \frac{2}{3}M^2_{\tilde{E}_i^c} , \tag{6}$$

$$M^2_{\tilde{D}_i^c} = \frac{5}{3}(M_0^U)^2 - \frac{2}{3}M^2_{\tilde{L}_i} , \tag{7}$$

where $M_{\tilde{Q}}$, $M_{\tilde{U}^c}$, $M_{\tilde{D}^c}$, $M_{\tilde{L}}$, and $M_{\tilde{E}^c}$ denote the scalar masses of the left-handed squark doublets, right-handed up-type squarks, right-handed down-type squarks, left-handed sleptons, and right-handed sleptons, respectively. Also, M_0^U is the univeral scalar mass, as in the mSUGRA. In the EWSUSY, $M_{\tilde{L}}$ and $M_{\tilde{E}^c}$ are both within 1 TeV, resulting in light sleptons. Especially, in the limit $M_0^U \gg M_{\tilde{L}/\tilde{E}^c}$, we have the approximated relations for squark masses: $2M^2_{\tilde{Q}} \sim M^2_{\tilde{U}^c} \sim M^2_{\tilde{D}^c}$. In addition, the Higgs soft masses $M_{\tilde{H}_u}$ and $M_{\tilde{H}_d}$, and the trilinear soft terms A_U, A_D and A_E can all be free parameters from the GmSUGRA [14, 16].

With the SM-like Higgs boson mass around 125 GeV, we can still have much lighter stops and gluino in the NMSSM than the MSSM, as explained in the Introduction. Thus, different from our previous EWSUSY work in the MSSM [14], in general, the squarks and gluino in the NMSSM can be either light below 1 TeV, or heavy about several TeV, beyond the reach of the current LHC. Let us classify the different combinations of M_3 and M_0, which would produce the very characteristic particle spectra of squarks and gluino in the following:

- Large M_3 and large M_0: all colored sparticles are definitely decoupled with masses around several TeV.

- Large M_3 and small M_0: similar to the case above.

- Small M_3 and large M_0: gluino is light around or below 1 TeV, while squarks are heavy. The mass squares of right-handed squarks are predicted to be approximately twice those of left-handed ones.

- Small M_3 and small M_0: all the colored sparticles could be light about $\sim 1 - 2$ TeV. Because the light first two generation squarks are disfavored by the null results of the

LHC SUSY searches, this case could survive only with the special sparticle spectra such as compressed ones or with the RPV.

The superpotential and SUSY breaking soft terms for the Higgs sector in the NMSSM are

$$W = \lambda S H_u H_d + \frac{\kappa}{3} S^3 \ , \tag{8}$$

$$V_{\rm soft} = m_{H_u}^2 |H_u|^2 + m_{H_d}^2 |H_d|^2 + m_S^2 |S|^2 + \left(\lambda A_\lambda S H_u H_d + \frac{1}{3} \kappa A_\kappa S^3 + h.c \right) \ . \tag{9}$$

After spontaneous electroweak symmetry breaking, the singlet scalar Higgs field S obtains a VEV, and then the effective μ term is generated dynamically, *i.e.*, $\mu_{\rm eff} = \lambda \langle S \rangle$. Also, in the decoupling limit and providing that there is no mixing between the Higgs doublets and singlet, we have the following tree-level Higgs boson mass

$$M_H^2 = m_Z^2 \cos^2 2\beta + \lambda^2 v^2 \sin^2 2\beta \ , \tag{10}$$

where $v^2 = (\langle H_u^0 \rangle)^2 + (\langle H_d^0 \rangle)^2 = (174 {\rm GeV})^2$. Comparing to the Higgs sector in the MSSM, we have an extra SM singlet Higgs field S and the mixings between Higgs doublets and singlet. To obtain a 125 GeV SM-like Higgs particle, one usually considered the small $\tan\beta \sim 2$ and large $\lambda \sim 0.6$ in the previous studies so that the new tree-level contribution can be large. Moreover, the proper doublet-singlet mixing can shift the Higgs boson mass by several GeV. As we know, the SM-like Higgs boson in the NMSSM can be either the lightest (H_1) or the second lightest (H_2) CP-even neutral Higgs boson. For the latter case it is more efficient to lift the SM-like Higgs boson mass up to $\sim$ 125 GeV while obtain the enhancement in di-photon channel through the suitable H/S mixing previously. To be concrete, with a lighter H_1 being singlet-like, the SM-like Higgs boson H_2 would be pushed up by the diagonalization of Higgs boson mass matrix [35]. Thus, a 125 GeV SM-like Higgs boson can be realized in the NMSSM without very heavy stops and gluino.

We display the characteristic mass hierarchy for the EWSUSY in the NMSSM in Fig. 1, where the dashed lines denote alternative cases. The squarks are heavy around several TeV, and gluino can be either heavy or light, although the light gluino is strongly constrained by the recent LHC SUSY searches. All the neutralinos, charginos, and sleptons, are light around several hundred GeV. The Higgsinos, which can be heavy, are also around electroweak scale, as the results of small $\mu_{\rm eff} \sim 100 - 300$ GeV from the following scan in the NMSSM. The features of Higgs sector are inspired by general NMSSM properties. At least two CP-even

(H_1 and H_2) and one CP-odd (A_1) neutral Higgs fields are light around 100 GeV, being H_u-like or S-like. The other heavy Higgs fields H_3, A_2 and $H^\pm$ being H_d-like can be either light around 500 GeV or heavy about several TeV. All these features will be explained in details in the following Section.

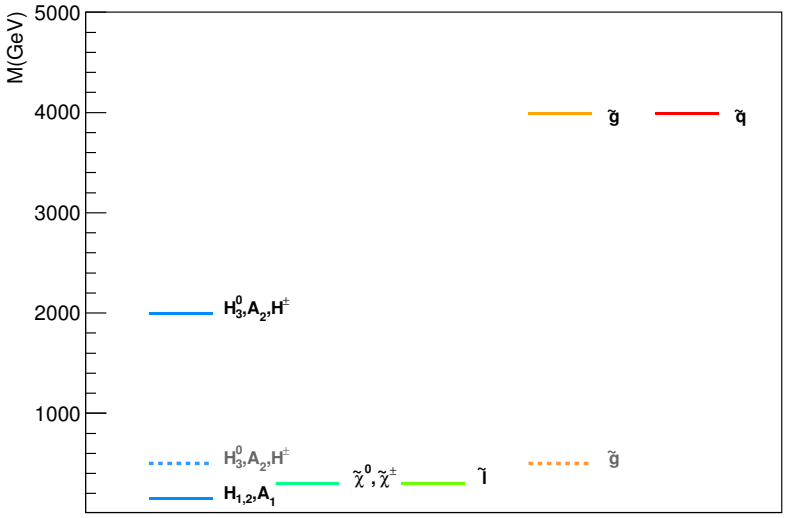

FIG. 1: The typical EWSUSY mass hierarchy for the particle spectra in the NMSSM. The dashed lines denote alternative cases.

B. SUSY Contributions to $(g_\mu - 2)/2$

The dominant SUSY contributions to the muon anomalous magnetic moment Δa_μ arise from the neutralino-smuon and chargino-sneutrino loops. And these contributions in the NMSSM are similar to the MSSM. In the NMSSM, the extra contribution would come from a very light pesdo-scalar Higgs boson ($\sim$ several GeV) [30], which can be neglected in the following discussions.

The contributions to Δa_μ from the neutralino-smuon and chargino-sneutrino loops are [27]

$$\Delta a_\mu^{\tilde{\chi}^0} = \frac{m_\mu}{16\pi^2}\sum_{i,m}\left\{-\frac{m_\mu}{12m^2_{\tilde{\mu}_m}}(|n^L_{im}|^2+|n^R_{im}|^2)F_1^N(x_{im}) + \frac{m_{\tilde{\chi}^0_i}}{3m^2_{\tilde{\mu}_m}}\mathrm{Re}[n^L_{im}n^R_{im}]F_2^N(x_{im})\right\}\ , \tag{11}$$

$$\Delta a_\mu^{\tilde{\chi}^\pm} = \frac{m_\mu}{16\pi^2}\sum_{k}\left\{\frac{m_\mu}{12m^2_{\tilde{\nu}_\mu}}(|c^L_k|^2+|c^R_k|^2)F_1^C(x_k) + \frac{2m_{\tilde{\chi}^\pm_k}}{3m^2_{\tilde{\nu}_\mu}}\mathrm{Re}[c^L_k c^R_k]F_2^C(x_k)\right\}\ , \tag{12}$$

where $i = 1,2,3,4,5$, $k = 1,2$, and $m = 1,2$ denote the mass eigenstates of neutralinos, charginos, and smuons, respectively. The kinematic variables are $x_{im} = m^2_{\tilde{\chi}^0_i}/m^2_{\tilde{\mu}_m}$, and $x_k = m^2_{\tilde{\chi}^\pm_k}/m^2_{\tilde{\nu}_\mu}$. The couplings are given by

$$n^L_{im} = \frac{1}{\sqrt{2}}(g_2 N_{i2} + g_1 N_{i1})X^*_{m1} - y_\mu N_{i3} X^*_{m2}\ , \tag{13}$$

$$n^R_{im} = \sqrt{2}g_1 N_{i1} X_{m2} + y_\mu N_{i3} X_{m1}\ , \tag{14}$$

$$c^L_k = -g_2 V_{k1}\ , \tag{15}$$

$$c^R_k = y_\mu U_{k2}\ , \tag{16}$$

where X_{m-}, N_{i-}, and U_{k-}/V_{k-} are the elements of the conventional mixing matrices for smuons, neutralinos, and charginos, respectively. In the gauge eigenstate bases, $\tilde{\chi}^0(G) = (-i\tilde{B}, -i\tilde{W}, \tilde{H}^0_d, \tilde{H}^0_u, \tilde{S})$, the i-th neutralino $\tilde{\chi}^0_j$ mass eigenstate is equal to $N_{ij}\tilde{\chi}^0_j(G)$. Similarly, we have $\tilde{\chi}^+_k = V_{kl}\tilde{\chi}^+_l(G)$, $\tilde{\chi}^-_k = U_{kl}\tilde{\chi}^-_l(G)$, and $\tilde{\mu}_m = X_{mn}\tilde{\mu}_n(G)$ in the gauge eigenstate bases $\tilde{\chi}^+(G) = (-i\tilde{W}, \tilde{H}^+_u)$, $\tilde{\chi}^-(G) = (-i\tilde{W}, \tilde{H}^-_d)$, and $\tilde{\mu}(G) = (\tilde{\mu}_L, \tilde{\mu}_R)$, respectively. Also, $y_\mu = m_\mu/(v\cos\beta)$ ($\sim m_\mu \tan\beta/v$ for large $\tan\beta$) is the muon Yukawa coupling. Loop functions $F^{N/C}_{1/2}(x)$ are normalized to 1 for $x = 1$. The concrete mixing matrices and loop functions were given in Refs. [26–29].

Because the magnetic moment operator is a chirality-flipping interaction, it is proportional to m_μ for external-leg chirality flipping (the first term in Eqs. (11) and (12)), and to Yukawa coupling for the internal-line chirality flipping (the second term in Eqs. (11) and (12)). The internal-line chirality-flipping terms would dominate since sparticles are much heavier than muon. The contributions from the neutralino-smuon and chargino-sneutrino loops can approximately be expressed as

$$\Delta a_\mu^{\tilde{\chi}^0\tilde{\mu}} \simeq \frac{1}{192\pi^2}\frac{m_\mu^2}{M^2_{SUSY}}\left(\mathrm{sgn}(\mu \mathrm{M}_1)g_1^2 - \mathrm{sgn}(\mu \mathrm{M}_2)g_2^2\right)\tan\beta\ , \tag{17}$$

$$\Delta a_\mu^{\tilde{\chi}^\pm\tilde{\nu}} \simeq \mathrm{sgn}(\mu \mathrm{M}_2)\frac{1}{32\pi^2}\frac{m_\mu^2}{M^2_{SUSY}}g_2^2\tan\beta\ . \tag{18}$$

Obviously, if all the relevant sparticles are at the same mass scale, the chargino-sneutrino loop contributions would dominate. So we have $\Delta a_\mu \sim 10^{-9} \left(\frac{100\ \text{GeV}}{M_{\text{SUSY}}}\right)^2 \tan\beta$ for $\text{sgn}(\mu M_2) > 0$. It was found in Ref. [28] that the 2σ bound on Δa_μ can be achieved for $\tan\beta = 10$ if four relevant sparticles are lighter than $600 - 700$ GeV. While for smaller $\tan\beta$ ($\sim$3), the lighter sparticles ($\lesssim 500$ GeV) are needed. All the relevant sparticles can be as light as several hundred GeV in the NMSSM with the EWSUSY. Thus, it would be very promising to explain the measured Δa_μ deviation.

III. NUMERICAL ANALYSES

A. Setup

In this subsection, we will use χ^2 statistic test to explore the EWSUSY parameter space in the NMSSM. We will take κ and μ_{eff} at M_{SUSY} as input parameters instead of the Higgs soft masses M_{H_u} and M_{H_d} at the GUT scale. So we have 13 free parameters in total as follows

$$M_{\tilde{L}},\ M_{\tilde{E}},\ M_1,\ M_2,\ M_0,\ A_0,\ A_E,\ A_\lambda,\ A_\kappa,\ \lambda,\ \kappa,\ \tan\beta,\ \mu_{\text{eff}}\ ,$$

where we assume $A_U = A_D = A_0$. Among these input parameters, λ, κ, $\tan\beta$, μ_{eff}, A_λ, A_κ, and A_0 are relevant to Higgs sector. $M_{\tilde{L}}$, $M_{\tilde{E}}$, μ_{eff}, M_1, and M_2 take control of the electroweak SUSY sector, and are set to be light around several hundred GeV. The input parameter ranges employed in numerical scan are the following: $M_0 \in (0, 3000)$ GeV, $M_1 \in (-1000, 1000)$ GeV, $M_2 \in (-1000, 1000)$ GeV, $M_{\tilde{L}} \in (0, 800)$ GeV, $M_{\tilde{E}} \in (0, 800)$ GeV, $\lambda \in (0, 0.7)$, $\tan\beta \in (1, 60)$. All the other parameters such as A_0 are just left free.

As explained in the Introduction, we consider three EWSUSY scenarios in the NMSSM. In Scenario I, the LSP neutralino is the only dark matter candidate, and then the dark matter relic density from WMAP experiment is involed in χ^2 analyses. In Scenario II, we assume the multi-component dark matter, and then there is an upper bound on the LSP neutralino relic density ($\Omega h^2 < 0.136$). Considering the variations in the local relic abundance, we rescale the WIMP-proton scattering cross section σ_p^{SI} to $\sigma_p^{SI} \times \Omega h^2/0.11$ so that the XENON100 upper limit [13] can be applied directly. The previous SUSY search constraints from the LEP and Tevatron are considered in Scenarios I and II as well. In Scenario III, R-parity is violated, and then there is no stable LSP. In general, the RPV

couplings are too small to shift the sparticle masses much [41]. Thus, we just ignore the RPV couplings in Renormalization Group Equation (RGE) running. In this scenario, we relax the LEP SUSY search constraints, and the requirement of the "lightestness" of the lightest neutralino, which means that any sparticle can be the LSP. There exist constraints for the RPV SUSY from the LEP2 [42] and LHC [5]. However, these existing bounds are highly model dependent. So we just neglect them in the following.

Taking into account the uncertainties for theoretical Higgs boson mass calculations, we require the SM-like Higgs boson mass to be within the range 125.5 ± 1.5 GeV. The SM-like Higgs boson at the LHC can be the lightest CP-even neutral Higgs boson H_1, or the second lightest CP-even one H_2, or even both of them. For the last case in which the two light CP-even neutral Higgs bosons are highly mass degenerate (say, $\Delta m < 2$ GeV), we combine these two Higgs boson productions and decays as Ref. [37] did to form one Higgs particle observed at the LHC. The effective mass and signal strength for decay channel XX are defined as follows

$$m_h^{XX} \equiv \frac{R_1^{XX} m_1 + R_2^{XX} m_2}{R_1^{XX} + R_2^{XX}} \ , \tag{19}$$

$$R_h^{XX} \equiv R_1^{XX} + R_2^{XX} \ , \tag{20}$$

where the Higgs signal strength is defined as

$$R_{XX} = \frac{\sigma(pp \to H)}{\sigma(pp \to H_{SM})} \times \frac{BR(H \to XX)}{BR(H_{SM} \to XX)} \ . \tag{21}$$

In the numerical study, the statistic test χ^2 is constructed in the following simple form

$$\chi^2 = \sum_i \frac{(x_i - x_i^0)^2}{\sigma_i^2} \ , \tag{22}$$

where x_i^0 and σ_i are respectively the experimental central value and error of the i-th observable, while x_i denotes the model prediction. We consider the following experimental results for χ^2 in the code: the Higgs signal strengths of main search channels from the ATLAS and CMS Collaborations, low energy phenomenological constraints including B physics, anomalous magnetic moment of the muon, and dart matter relic density (for Scenario I only). All these constraints are listed in Table I. Thus, the degree of freedom is 15 for Scenario I and 14 for Scenarios II and III.

In our numerical study, the NMSSMTools [43] is used for the RGE runnig and the calculations of low energy phenomenological constraints. We have adapted the source code to

	25 fb^{-1}	$\gamma\gamma$	1.65 ± 0.32
	25 fb^{-1}	ZZ	1.7 ± 0.45
ATLAS^{7+8}	25fb^{-1}	WW	1.01 ± 0.31
	18fb^{-1}	Vbb	-0.4 ± 1.0
	18fb^{-1}	$\tau\tau$	0.7 ± 0.7
	25 fb^{-1}	$\gamma\gamma$	1.11 ± 0.31(Cut-based)
	25 fb^{-1}	ZZ	0.91 ± 0.27
CMS^{7+8}	24 fb^{-1}	WW	0.76 ± 0.21
	17 fb^{-1}	Vbb	1.3 ± 0.65
	24 fb^{-1}	$\tau\tau$	1.1 ± 0.4
BR($B \to X_s\gamma$)			$(3.55 \pm 0.256) \times 10^{-4}$ [10]
BR($B_s^0 \to \mu^+\mu^-$)			$3.2^{+1.5}_{-1.2} \times 10^{-9}$ [6]
BR($B \to \tau\nu_\tau$)			$(1.67 \pm 0.3) \times 10^{-4}$ [10]
Δa_μ			$(2.87 \pm 0.8) \times 10^{-9}$ [11]
Ωh^2			0.1157 ± 0.0023 [12]

TABLE I: The LHC Higgs signal strengths [4] after Moriond 2013, and the other experimental constraints.

accomodate the general SUSY breaking soft terms in the GmSUGRA. The LSP neutralino relic density and LSP neutralino-proton spin-independent scattering cross section are calculated via the micrOMEGAs [44] implemented in the NMSSMTools package. For simplicity, we take the top quark pole mass as 173.5 GeV. To be more efficient in computation, we use the Markov Chain Monte Carlo (MCMC) technique for parameter space scan.

B. Numerical Results

We scan the whole parameter space systematically, and obtain the minimal χ^2/DOF 10.2/15, 9.6/14, and 9.2/14 respectively in Scenarios I, II, and III. We list the three best-fit points in Table II. The summarized results are shown in two-dimensional (2D) panels in Figs. 2, 3, and 4 for Scenarios I, II, and III, respectively. We display the 1σ ($\Delta\chi^2 = \chi^2 - \chi^2_{\rm min} < 2.3$), 2σ ($\Delta\chi^2 < 6.2$), and 3σ ($\Delta\chi^2 < 11.8$) regions in every 2D distribution with the other

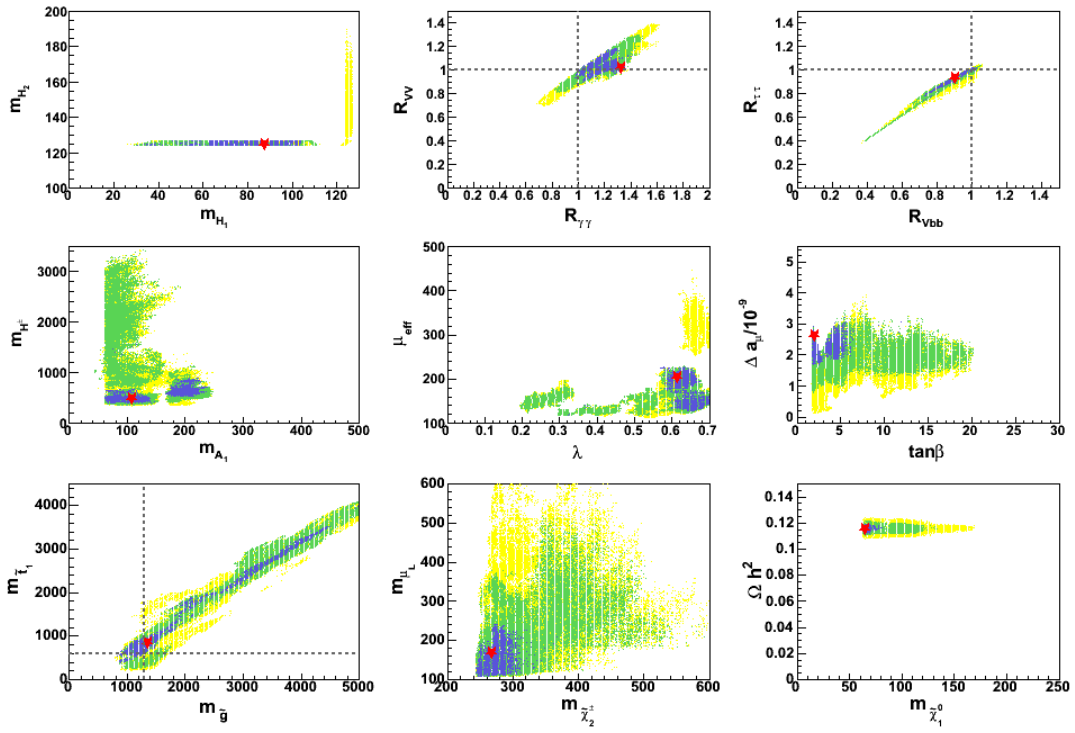

FIG. 2: Summary results for the parameter space scan in Scenario I with $\chi^2_{min}/\mathrm{DOF} = 10.2/15$. In all the panels, the best-fit point is marked with red pentagram. 1σ, 2σ, and 3σ regions are colored in purple, green, and yellow, respectively. All the particle masses and $\mu_{\rm eff}$ are displayed in unit GeV. The naive bounds from SUSY searches at the LHC are also shown in $m_{\tilde{g}} - m_{\tilde{t}_1}$ panel, with 1.3 TeV for gluino and 600 GeV for light stop.

parameters marginalized. For all three scenarios, we discuss the NMSSM input parameters, the Higgs sector, and the most relevant sparticle masses. Moreover, we explain the LSP neutralino in details for Scenarios I and II, and comment on the possible LSP for Scenario III.

- The NMSSM Input Parameters and $\Delta a_\mu - \tan\beta$

  From the $\lambda - \mu_{\rm eff}$ and $\Delta a_\mu - \tan\beta$ plots in Figs. 2, 3, and 4, we find that small $\mu_{\rm eff}$ ($\lesssim 300$ GeV) are prefered in all three scenarios. In Scenario I, small $\tan\beta$ and large λ are favored as expected from the 1σ region of χ^2 annalyses. The SM-like Higgs boson is the second lightest CP-even neutral Higgs boson H_2, whose mass can be lifted by the large tree-level contribution and pushing up effect. Thus, the light stop and

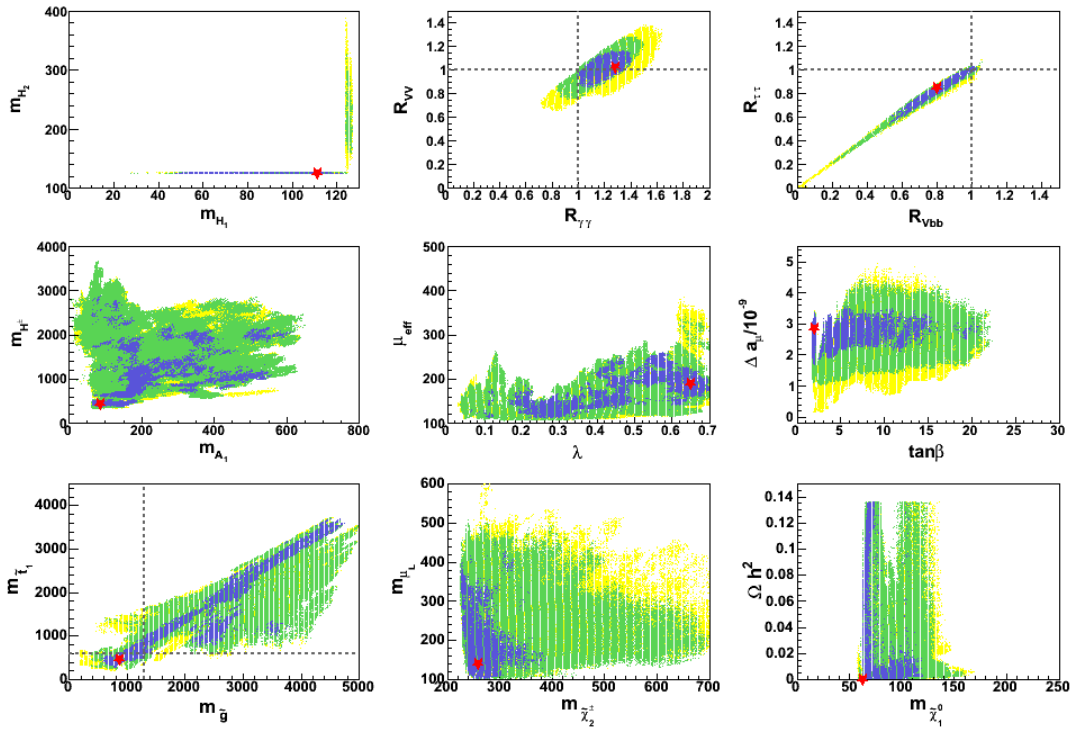

FIG. 3: Summary results for the parameter space scan in Scenario II with $\chi^2_{min}/\mathrm{DOF} = 9.6/14$. In all the panels, the best-fit point is marked with red pentagram. 1σ, 2σ, and 3σ regions are colored in purple, green, and yellow, respectively. All the particle masses and $\mu_{\rm eff}$ are displayed in unit GeV. The naive bounds from SUSY searches at the LHC are also shown in $m_{\tilde{g}} - m_{\tilde{t}_1}$ panel, with 1.3 TeV for gluino and 600 GeV for light stop.

gluino can indeed be light $\lesssim 1$ TeV in this regime. Previously, this case has been studied extensively. However, in Scenarios II and III which relax the dark matter relic abundance requirement, we obtain the other interesting parameter space: 1σ region of χ^2 analyses covers the wider ranges of $\tan\beta$ and λ, for example, $\tan\beta$ from 2 to 20 and λ from 0.1 to 0.7 in Scenario II. Except for the well-investigated combination, the larger $\tan\beta$ and smaller λ regime is also quite promising: Δa_μ can be increased effectively due to the larger $\tan\beta$, and the SM-like Higgs boson (H_2) mass can still be lifted by the pushing up effect because of the relatively large A_λ.

- Higgs Sector

  For Higgs sector, we present the plots for $R_{\gamma\gamma} - R_{VV}$ and $R_{Vbb} - R_{\tau\tau}$, as well as the

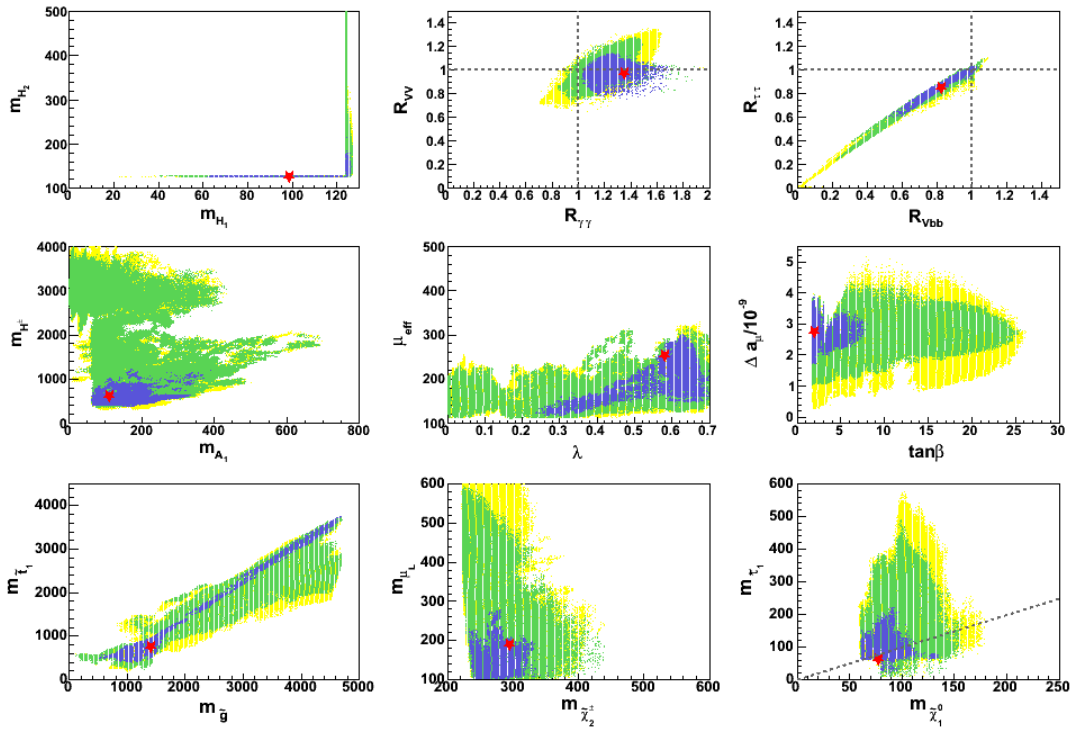

FIG. 4: Summary results for the parameter space scan in Scenario III with $\chi^2_{min}/\text{DOF} = 9.2/14$. In all the panels, the best-fit point is marked with red pentagram. 1σ, 2σ, and 3σ regions are colored in purple, green, and yellow, respectively. All the particle masses and μ_{eff} are displayed in unit GeV. Dashed line in $m_{\tilde{\chi}_1^0} - m_{\tilde{\tau}_1}$ panel is the seperation line with $m_{\tilde{\chi}_1^0} = m_{\tilde{\tau}_1}$.

masses of m_{H_1}, m_{H_2}, m_{A_1}, and $m_{H^\pm}$ (H_3, A_2 and $H^\pm$ are almost mass degenerate since they are all H_d-like.). In the m_{H_1}-m_{H_2} planes, the horizontal lines correspond to the cases in which the second lightest CP-even neutral Higgs boson H_2 is SM-like and has a mass in the range [124, 127] GeV, while the vertical lines correspond to the cases of the lightest CP-even neutral Higgs boson H_1 being SM-like. At the intersection, these two Higgs bosons will all contribute to the LHC signals together in the manner presented in the previous subsection. From the 1σ region of χ^2 analyses, we obtain that the second lightest CP-even Higgs boson is more likely to be the SM-like Higgs boson discovered at the LHC, as pointed out in many previous literatures. The only exception is a small region in Scenario III where H_1 is the SM-like Higgs boson and H_2 is still lighter than about 180 GeV. Thus, in the most favourable parameter space, we have another lighter Higgs boson with mass less than 125 GeV, which has reduced couplings with the SM

particles. The corresponding signal strengths for dominant decay channels of the Higgs boson discovered at the LHC are presented in the $R_{\gamma\gamma} - R_{VV}$ and $R_{Vbb} - R_{\tau\tau}$ planes. The 1σ region generically predicts that $R_{\gamma\gamma}$ ($R_{Vbb}/R_{\tau\tau}$) is a little bit larger (smaller) than 1.0. In the $m_{A_1} - m_{H^\pm}$ plane, we can see that A_1 is singlet-like and always lighter than 800 GeV, and the smaller values of m_{A_1} are more favored. The masses of the H_d-like Higgs bosons have wide ranges from a few hundred GeV to several TeV, and can be lighter than 1 TeV for small $\tan\beta \sim 2$. However, when $\tan\beta$ increases, the masses of the H_d-like Higgs bosons will increase as well since they are approximately proportional to $\tan\beta$, rendering heavier A_2, H_3, and $H^\pm$. The more specific discussions about large $\tan\beta$ regime will be given in subsection IV C 2. It is obvious that the 1σ regions are smaller in Scenario I compared to the Scenarios II and III since the requirement of the correct dark matter relic density imposes some constraints on the LSP components. The appropriate singlino fraction in the LSP neutralino is required since it is dominantly Higgsino like in Scenario I. We will comment on it in the following analyses about the LSP.

- Relevant Sparticle Masses

  As for sparticles, we present two panles, one ($m_{\tilde{g}} - m_{\tilde{t}_1}$) for colored sparticles and the other ($m_{\tilde{\chi}_2^\pm} - m_{\tilde{\mu}_L}$) for the representative sparticles in electroweak SUSY sector which invole in Δa_μ. The narrow strips corresponding to 1σ regions of χ^2 analyses in $m_{\tilde{g}} - m_{\tilde{t}_1}$ planes indicate that the colored sparticles such as light stop and gluino could be either heavy about several TeV or relatively light $\lesssim 1$ TeV. We observe that the light stop could be as light as 400 GeV in 1σ regions. The light stop ($\lesssim 600$ GeV) regions could only be viable with small $\tan\beta$ and large λ since the large tree-level contributions to the SM-like Higgs boson mass are needed. When $\tan\beta$ increases, the larger light stop mass is required to compensate the reduction of the tree-level contribution to the SM-like Higgs boson mass. Since the LHC has given stringent constraint on the colored sparticle productions, we also show the naive bounds on the light stop and gluino masses for reference. Just keep it in mind that the light stop lighter than ~ 600 GeV and gluino lighter than ~ 1.3 TeV may be excluded with the LHC searches. Actually, we do not need to worry about this issue in the EWSUSY since the following analyses of the LHC neutralino/chargino and slepton searches will

push $\tan\beta$ to be large which corresponds to heavy squarks and gluino.

In the $m_{\tilde{\chi}_2^\pm} - m_{\tilde{\mu}_L}$ plots, $\tilde{\chi}_2^\pm$ and $\tilde{\mu}_L$ are always as light as several hundred GeV, which is required by the EWSUSY. Because Higgsinos are always lighter than about 300 GeV by the virtue of small $\mu_{\rm eff}$, $\tilde{\chi}_2^\pm$ is Wino like in most of the parameter space. When $\tilde{\chi}_2^\pm$ is very light, Wino and Higgsino would have large mixing. Given a small $\tan\beta$, very light smuon and Wino are prefered by Δa_μ. Such light charginos and sleptons may be excluded from the LHC SUSY searches [45], which will be discussed in the next Section.

We do not present the neutralino sector here, since it is just trivial. Five neutralinos are all light within several hundred GeV. In the basis $\tilde{\chi}^0 = (-i\tilde{B}, -i\tilde{W}, \tilde{H}_d^0, \tilde{H}_u^0, \tilde{S})$, the neutralino mass matrix is [31]

$$\mathbf{M}_{\tilde{\chi}^0} = \begin{pmatrix} M_1 & 0 & -\frac{g_1 v_d}{\sqrt{2}} & \frac{g_1 v_u}{\sqrt{2}} & 0 \\ & M_2 & \frac{g_2 v_d}{\sqrt{2}} & -\frac{g_2 v_u}{\sqrt{2}} & 0 \\ & & 0 & -\mu_{\rm eff} & -\lambda v_u \\ & & & 0 & -\lambda v_d \\ & & & & 2\kappa s \end{pmatrix} .$$

We have small $\mu_{\rm eff}(=\lambda s)$, which renders a lighter singlino due to $2\kappa s \sim 2\frac{\kappa}{\lambda}\mu_{\rm eff}$. In other words, the singlino is lighter than about 200 GeV, and has large mixings with two light Higgsinos. Since the Bino and Wino masses are free in principle, they could be either much heavier than $\sim 200 - 300$ GeV, or as light as ~ 300 GeV. When they are heavier, the typical neutralino order from light to heavy is $\tilde{H}_{u/d}$, $\tilde{H}_{d/u}$, $\tilde{S}$, $\tilde{B}$, $\tilde{W}$. In most cases, the fisrt three states would have large mixings, while the last two are dominated by Bino and Wino respectively. Thus, we have almost mass degenerate $\tilde{\chi}_5^0$ and $\tilde{\chi}_2^\pm$ being Wino-like. On the other hand, when five neutralinos are all very light, there exist large mixings among them. All these features would take effects in the collider searches for electroweak SUSY sector.

- The Lightest Supersymmetric Particle (LSP)

  We show the LSP neutralino relic density for Scenarios I and II respectively in Figs. 2 and 3. It is obvious that the WMAP range for dark matter relic density dominates the χ^2 values in Scenario I. Just a narrow strip survives there with the LSP mass

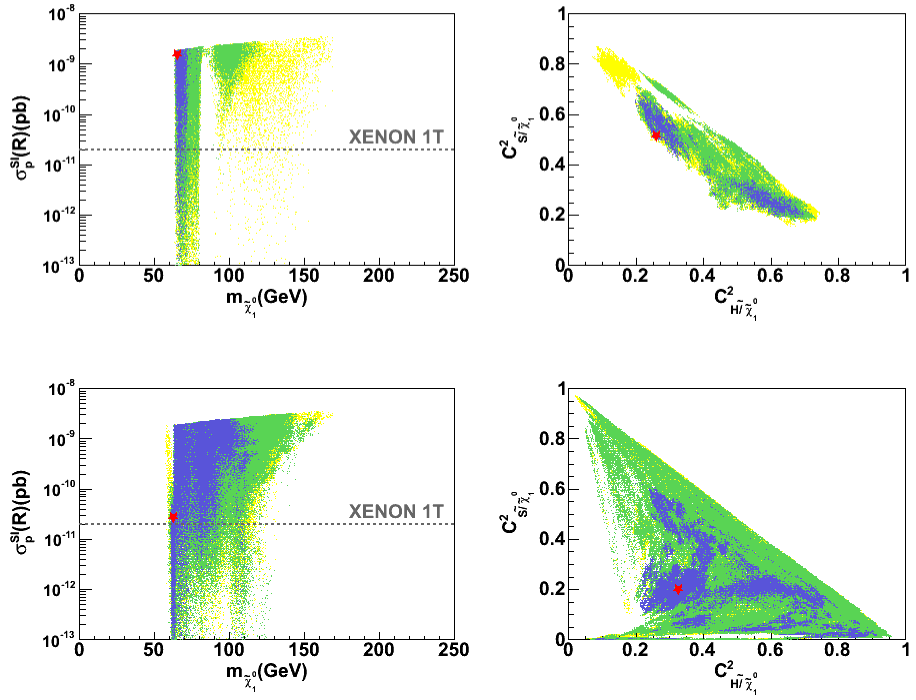

FIG. 5: The upper and down two plots are for Scenarios I and II, respectively. In the left two plots, we present the rescaled spin-independent LSP neutralino-proton scattering cross section $\sigma_p^{SI}(R) = \sigma_p^{SI} \times \Omega h^2/0.11$ versus the LSP neutralino mass. The expected XENON1T sensitivity ($\sim 10^{-11}$pb) is shown as well. In the right two plots, we give the LSP Higgsino and singlino components in $C^2_{\tilde{H}/\tilde{\chi}_1^0} - C^2_{\tilde{S}/\tilde{\chi}_1^0}$ planes.

range $\sim [60,\ 80]$ GeV in 1σ region of χ^2 analyses. And in Scenario II, 1σ region maps to wider LSP mass range, from 60 GeV to 120 GeV, and the LSP neutralino relic density could be very small due to its large Higgsino component. We can write the LSP neutralino mass eigenstate in terms of gauge eigenstates

$$\tilde{\chi}_1^0 = C_{\tilde{B}/\tilde{\chi}_1^0}(-i\tilde{B}) + C_{\tilde{W}/\tilde{\chi}_1^0}(-i\tilde{W}) + C_{\tilde{H}_d/\tilde{\chi}_1^0}\tilde{H}_d + C_{\tilde{H}_u/\tilde{\chi}_1^0}\tilde{H}_u + C_{\tilde{S}/\tilde{\chi}_1^0}\tilde{S}\ . \tag{23}$$

Higgsinos have large annihilation cross sections into the SM particles, and then the relic density for the Higgsino dominant LSP neutralino will be smaller than the observed unless the LSP neutralino is a few TeV. Also, Higgsinos have large scattering cross sections with the SM particles. Thus, some singlino components are needed to obtain the correct dark matter relic density and satisfy the XENON100 experimental bound.

We display the spin-independent LSP neutralino-proton scattering cross section and the LSP Higgsino and singlino components in Fig. 5. Because of the large Higgsino component in the LSP, the XENON100 experiment would impose tight constraints on the LSP neutralino-proton scattering processes. One can see that the best-fit point in Scenario I is just below the current bound curve. We also show the expected XENON1T sensitivity ($\sim 10^{-11}$pb) in the plots. The majority of parameter space could be detected at the XENON1T in the next a few years. The $C^2_{\tilde{H}/\tilde{\chi}^0_1} - C^2_{\tilde{S}/\tilde{\chi}^0_1}$ (with $C^2_{\tilde{H}/\chi^0_1} \equiv C^2_{\tilde{H}_u/\chi^0_1} + C^2_{\tilde{H}_d/\chi^0_1}$) plots differs in Scenarios I and II. In Scenario I, the LSP neutralinos are almost composed of Higgsinos and singlino only, while the moderate Wino and/or Bino components may invole in Scenario II. As expected, the moderate to large singlino component in the LSP is required in Scenario I.

In Scenario III due to RPV, the heavy sparticles will finally decay into the SM particles through the RPV superpotential terms. We present a plot of $m_{\tilde{\chi}^0_1} - m_{\tilde{\tau}_1}$ in Fig. 4. In the EWSUSY, the LSP could be $\tilde{\chi}^0_1$, $\tilde{\tau}_1$, or $\tilde{\nu}_\tau$. The mass order among them would influence the cascade decays of the sparticles produced at the colliders, resulting in different signatures with the same heavy sparticle spectra.

In summary, we have two different viable regimes: (1) the light stop and gluino are relatively light within 1 TeV. And then the small $\tan\beta$ and large λ are prefered by the 125 GeV SM-like Higgs boson, and somewhat lighter neutralinos/charginos and smuon/muon-sneutrino are required to make up Δa_μ; (2) The squarks and gluino are all heavy around several TeV. With the substantial radiative corrections to the SM-like Higgs boson mass from heavy stops, the relatively larger $\tan\beta$ is favored by Δa_μ confronted with the constraints from the LHC neutralino/chargino and slepton searches, which will be discussed in the following.

IV. THE SEARCHES FOR THE ELECTROWEAK SUSY SECTOR AT THE COLLIDERS

A. The EWSUSY Particle Spectra in the NMSSM Inspired by Δa_μ

Before the further phenomenological studies, we would like to summarize all the above theoretical and experimental results:

- In the NMSSM, to obtain a 125 GeV SM-like Higgs boson, we have small $\mu_{\rm eff} \sim 100 - 300$ GeV in the most favourable regions. Thus, we have at least three light neutralinos ($\tilde{H}_u,\ \tilde{H}_d,\ \tilde{S}$), and one light chargino ($\tilde{H}^{\pm}$) around 100 GeV to 300 GeV.

- In Higgs sector, the second lightest CP-even neutral Higgs boson is SM-like in 1σ regions of χ^2 analyses in Scenarios I and II, and in almost all the 1σ regions in Scenario III. The point is that the diagonalization of Higgs boson mass matrix would push up the SM-like Higgs boson mass. With the lightest CP-even and CP-odd Higgs bosons being singlet-like, we have three light Higgs bosons H_1, H_2, and A_1. As for the other three H_d-like Higgs bosons, they would be either light within 1 TeV in the small $\tan\beta$ and large λ regime, or heavy about several TeV in large $\tan\beta$ regime which will be argued to be more interesting in subsection IV C 2 from the LHC SUSY searches.

- The EWSUSY motivated by Δa_μ predicts the light neutralinos, charginos, and sleptons (either left-handed, or right-handed, or both of them), which form the complete light electroweak SUSY sector imposed by the general NMSSM.

- In principle, the squarks and gluino could be either light or heavy, which depend on the specific input parameters. We will show that they are indeed heavy from the LHC SUSY searches, as predicted from the EWSUSY.

As one can see from the last Section, the light electroweak SUSY sector is definitely needed for the EWSUSY, while light stop and gluino in the NMSSM could be somewhat lighter than those in the MSSM due to the extra contributions to the SM-like Higgs boson mass from the tree-level F-term and pushing up effect. However, light stop and gluino are strongly disfavored when the LHC SUSY search results are taken into account. Thus, we come back to our original EWSUSY picture: the squarks and/or gluino are heavy about several TeV, and out of the current LHC reach. After the following dedicated LHC SUSY search studies, we will comfirm that this assumption is indeed valid. Thus, we will concentrate on the searches for electroweak SUSY sector: neutralinos, charginos, and sleptons, with the colored sparticles totally decoupled.

The sparticles in electroweak SUSY sector have much smaller production cross sections at the LHC than squarks/gluino, and they are only mainly pair produced in electroweak processes through s channels via electroweak gauge boson exchanges. For Wino with mass

around 200–500 GeV, the Wino-like neutralino-chargino pair production cross section varies from ~ 0.2 pb to ~ 0.002 pb at the LHC with $\sqrt{s} = 7$ TeV, while the slepton pair production has about 50 times smaller cross section. The corresponding cross sections will increase by several times at the LHC-14. The ATLAS and CMS Collaborations have performed the searches for the pair productions of neutralinos/charginos and sleptons [45]. They focused on the Wino-like chargino-neutralino $\tilde{\chi}_2^0\tilde{\chi}_1^\pm$ pair production and the slepton $\tilde{l}\tilde{l}^*$ pair production with Bino-like $\tilde{\chi}_1^0$. Results are interpretated in simplified models. The specific decay chains are assumed for Winos: $\tilde{\chi}_2^0 \to l\tilde{l} \to ll\tilde{\chi}_1^0$ and $\tilde{\chi}_1^\pm \to l\tilde{\nu} \to l\nu\tilde{\chi}_1^0 (l = e, \mu, \tau)$ for sleptons lighter than Winos; and $\tilde{\chi}_2^0 \to Z^{(*)}\tilde{\chi}_1^0$ and $\tilde{\chi}_1^\pm \to W^{\pm(*)}\tilde{\chi}_1^0$ for heavy sleptons. The signatures of tri-leptons or same-sign di-leptons with missing energy would be produced in the cascade decays. The first case would produce quite a few leptons, while less leptons are produced and large SM backgrounds involve in the second case. τ-enriched scenario is also considered, assuming the light right-handed sleptons and $\tilde{\chi}_1^\pm$ decays through its Higgsino component. In these simplified topologies, Winos with mass less than 600 GeV have been excluded at 95% C.L. for the lighter sleptons and the LSP lighter than 200 GeV. The mass upper limit is reduced to ~ 320 GeV in the absence of light sleptons. In addition, chargino and slepton pair productions are explored in the opposite-sign lepton-pair search channel. Interpreted in simplified models, the chargino mass can be explored up to ~ 400 GeV, and the left-handed slepton masses are explored up to ~ 200 GeV.

However, these bounds on sparticle masses can not be applied directly to the concrete models since the productions and decays are much more complicated. First of all, we need to consider the whole light electroweak SUSY sector, such as Higgsinos, sleptons, Bino, and Winos. So we have more signal sources. Second, the decay chains would become longer, and various decay chains would entangle with each other. Generally speaking, heavy neutralinos and chargino would decay into lighter ones accompanied with electroweak gauge bosons or light Higgs bosons. With sleptons lighter than them, the slepton channels would be dominant decay modes and give rise to rich leptons in final states. Taking the best-fit point of Scenario I as an example, we have all the neutralinos and charginos lighter than 300 GeV, and all the sleptons lighter than ~ 200 GeV. The neutralinos and charginos are all well mixed. With a quite light $\tilde{\tau}_1$ (93 GeV), $\tilde{\chi}_1^\pm$, $\tilde{\chi}_2^0$, and $\tilde{\chi}_3^0$ will all decay into $\tilde{\tau}_1$ with $\sim 100\%$ branching ratios through their Higgsino components. However, the small mass splitting between $\tilde{\tau}_1$ and the LSP, which leads to soft decay products, would block majority of the signals. $\tilde{\chi}_4^0$, $\tilde{\chi}_5^0$, and

$\tilde{\chi}_2^\pm$ are heavier and have enough phase space to decay to the lighter sleptons and on-shell gauge bosons, which will give rise to rich leptons in final states. $\tilde{\chi}_2^\pm$ will decay into the light left-handed sleptons (with an exception of $\tilde{\tau}_R$ since Higgsino component in $\tilde{\chi}_2^\pm$ would decay into lighter $\tilde{\tau}_R$), the lighter chargino or neutralinos, and the $\tilde{\chi}_1^\pm$ and light Higgses with branching ratios 40%, 45%, and 11%, respectively. $\tilde{\chi}_5^0$ will decay into $\tilde{\chi}_1^\pm W^\mp$ and sleptons respectively with branching ratios 32% and 40%, and decay into $\tilde{\chi}_i^0 Z$ and $\tilde{\chi}_i^0 H/A$ with small branching ratios. The longer cascade decay chains would give rise to more, although softer, leptons. The significant signature would be multi-leptons (including τ). The more detailed features in the search for electroweak SUSY sector will be discussed in subsection IV D. In next subsection, we will apply the current LHC SUSY search results to our sampled points. Because the dominant signals come from the decays of heavier neutralinos/chargino and then the masses of left-handed sleptons would modify the decay modes drastically, we will interpret our results in terms of $m_{\tilde{\chi}_2^\pm}$ (Wino mass typically) and $m_{\tilde{\mu}_L}$, which are also the most important particles in SUSY contribution to Δa_μ in our study.

B. The LHC SUSY Search Bounds

In this subsection, we apply the LHC neutralino/chargino and slepton search results to check our sampling points. The 8 TeV-9.2 fb^{-1} results from the CMS Collaboration and the 8 TeV-13 fb^{-1} results from the ATLAS Collaboration are employed. We consider the following analysis procedure: for each point, we generate events via Monte Carlo tools, and then apply the experimental selections and cuts to them. After we obtain the effective contribution in every signal region ($N_{\rm sig.}$), we compare the model prediction with the 95% C.L. upper limit ($N_{\rm U.L.}$) provided by the experimental Collaborations. If any new contribution is larger than the limit ($N_{\rm sig.}/N_{\rm U.L.} > 1$), this point or model is excluded.

MadGraph5 [46] is used to generate parton-level events and Pythia6.4 [47] is employed to perform parton shower and hadronization. Then events are passed to PGS4 [48] for detector simulation. With all the squarks and gluino so heavy, we only generate the processes for $\tilde{\chi}\tilde{\chi}$ and $\tilde{l}\tilde{l}$ pair productions, where $\tilde{\chi}$ includes all the neutralinos/charginos and $\tilde{l}$ represents all the sleptons. Instead of the complete calculations for every model points, a NLO k-factor of 1.2 [49] is taken for simplicity. Because the LSP would influence the sparticle cascade decay final states a lot, we will study three scenarios separately. For Scenario III with RPV,

Pythia8 and Delphes [50] are employed instead of Pythia6.4 and PGS4.

For Scenario I, we have checked ~ 1300 points which have Δa_μ in 2σ range. Results are shown in Fig. 6. In the left plot, we present the signal to upper limit ratio ($N_{\rm sig.}/N_{\rm U.L.}$) respect to the $\tilde{\chi}_2^\pm$ mass, with $m_{\tilde{\mu}_L}$ coded in color. One can see that most points have been excluded by current LHC SUSY searches. No points with $\tilde{\chi}_2^\pm$ lighter than ~ 350 GeV survive here. And all the survived points have relatively heavier $\tilde{\mu}_L \gtrsim 350$ GeV. In order to make it clear, we display the survived points in the $m_{\tilde{\chi}_2^\pm} - m_{\tilde{\mu}_L}$ plane with colored markers for Δa_μ in the right plot, while coloring the excluded ones in black. One can see the values of Δa_μ through maker's colors. The survived points mainly distribute in the small region with $M_{\tilde{\chi}_2^\pm} \lesssim M_{\tilde{\mu}_L}$ or $\tilde{\chi}_2^\pm$ and $\tilde{\mu}_L$ are very mass degenerate. In this region, because sleptons are generally heavier than neutralinos and charginos, the pair-produced neutralinos and charginos will decay to lighter neutralinos/chargino and electroweak gauge bosons, corresponding to the simplified model with chargino and second neutralino decaying to the LSP through on shell or off shell W/Z bosons. The difference is that the cascade decay chains are longer here, resulting more on-shell or off-shell gauge bosons in final states. Because the masses of Wino and sleptons are pushed up by the LHC SUSY search results, we obtain large $\tan\beta$ ($\gtrsim 11$) enforced by Δa_μ for survived points. Now with such large $\tan\beta$, the squark and gluino masses are automatically pushed up to several TeV in requirement of the 125 GeV SM-like Higgs boson mass. Three survived benchmark points are given in Table III, with branching fractions of dominant decay modes for relevant sparticles displayed as well. Because it is impossible to list all the decay modes for every sparticle, we just present some common and important ones. Thus, some decay modes, which would be dominant in specific cases, may be missing in our table. The complete information could also be obtaind by simple physical estimation.

As for Scenario II, the LHC SUSY search constraints would be applied in the similar way as in Scenario I due to the similar particle spectra in light of the SM-like Higgs boson mass and Δa_μ. We have also checked ~ 1300 sampled points with Δa_μ in 2σ range in Scenario II, and present the results in Fig. 7. We can see that there exist two main viable regions in the $m_{\tilde{\chi}_2^\pm} - m_{\tilde{\mu}_L}$ plane. One corresponds to the points with $\tilde{\chi}_2^\pm$ heavier than $\tilde{\mu}_L$, and in this region the $\tilde{\chi}_2^\pm$ mass is pushed up to about 450 GeV since the decay chains mediated by the light sleptons have large signal significances in the tri-lepton or same-sign di-lepton search channels. The other region locates at the up-left corner with $M_{\tilde{\chi}_2^\pm} \lesssim M_{\tilde{\mu}_L}$, and no

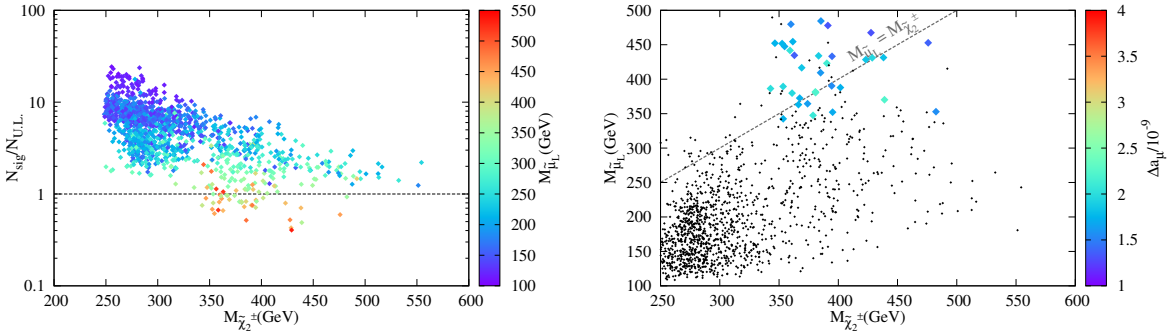

FIG. 6: **Left**: The signal to U.L. ratio ($N_{\rm sig.}/N_{\rm U.L.}$) versus $M_{\tilde{\chi}_2^\pm}$ for all the sampled points in Scenario I. **Right**: $M_{\tilde{\chi}_2^\pm} - M_{\tilde{\mu}_L}$ plane. The dead points are in black, and the survived ones are marked with color suggesting values of Δa_μ.

definite bound on $m_{\tilde{\chi}_2^\pm}$ can be obtained. So, unlike the Scenario I, the very light $\tilde{\chi}_2^\pm$ (~ 230 GeV) are still available in this region. Similar to Scenario I, almost all the viable points have larger $\tan\beta$ ($\gtrsim 8$) and heavy squarks/gluino. We also give three survived benchmark points within 2σ range of χ^2 analyses in Table IV.

Also, we find an interesting exception in Scenario II. One single point with $\tan\beta = 2.5$ survives. From the above discussion, $\mu_{\rm eff}$ is larger than M_2 for this point. The LHC signals mainly come from heavier Higgsinos decays. However, Higgsinos have relatively smaller production cross sections, resulting in slightly reduced signals. Strictly speaking, we should present this point with $m_{\tilde{\chi}_1^\pm}$ instead of $m_{\tilde{\chi}_2^\pm}$ since $\tilde{\chi}_1^\pm$ is Wino-like here. Thus, this point just corresponds to the up-left region in the $m_{\tilde{\chi}_2^\pm} - m_{\tilde{\mu}_L}$ plot of Fig. 7. For reference, we present this special point as Point IV in Table IV.

However, in Scenario III, the LHC phenomenology is somewhat different due to R-parity violation. The LSP is not stable, and then can be the lightest neutralino, light stau, or tau-snetrino [41]. Also, there is no missing energy for sparticle productions and decays at colliders. The standard RPV superpotential in the NMSSM with Z_3 symmetry is

$$W_{\not R} = \lambda_i^\mu S H_u L_i + \frac{1}{2}\lambda_{ijk} L_i L_j E_k^c + \lambda'_{ijk} L_i Q_j D_k^c + \frac{1}{2}\lambda''_{ijk} U_i^c D_j^c D_k^c \ . \tag{24}$$

For simplicity, we do not consider λ_i^μ here, and take the other RPV trilinear couplings to be smaller than about 10^{-3} which will not change the sparticle mass spectra. Thus,

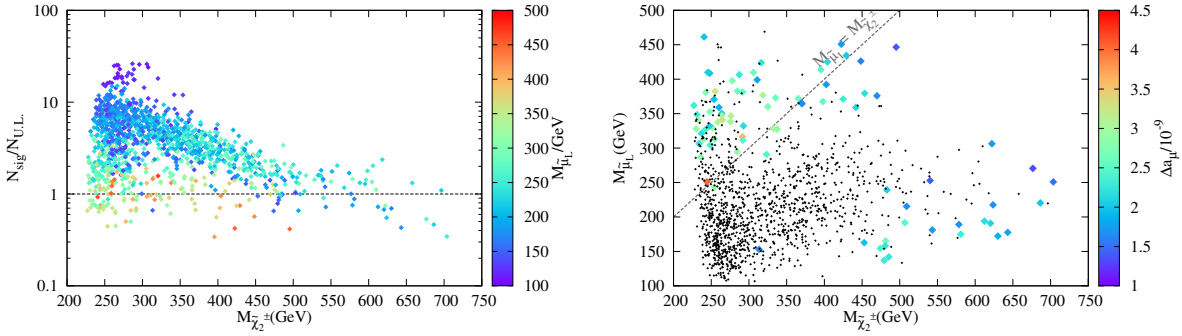

FIG. 7: **Left**: The signal to U.L. ratio ($N_{\rm sig.}/N_{\rm U.L.}$) versus $M_{\tilde{\chi}_2^\pm}$ for all the sampled points in Scenario II. **Right**: $M_{\tilde{\chi}_2^\pm} - M_{\tilde{\mu}_L}$ plane. The dead points are in black, and the survived ones are marked with color suggesting values of Δa_μ.

the sparticles will be dominantely produced in pairs (The RPV couplings are too small to render the resonant sparticle productions.). All the cascade decay chains will end in the SM particles due to the RPV superpotential terms. The RPV coulings λ, λ', and λ'' respectively correspond to the leptonic, semileptonic and hadronic decays, giving different final states.

We take only one RPV coupling (say, λ_{121}, λ'_{311}, or λ''_{212}) to be non-zero at one time. Turning on λ will bring too many lepton signals which are strongly constrained. Thus, we will just consider the non-zero λ' and λ'' here. For simplicity, we explore the RPV effects with several benchmark points, instead of performimg a complete scan over parameter space as in the first two Scenarios. With $\lambda'_{311} \neq 0$, the $\tilde{\chi}_1^0$-LSP will decay to one τ lepton and two jets ($\tilde{\chi}_1^0 \to \tau^- u\bar{d}/\tau^+\bar{u}d$), which gives an extra lepton while eliminates the original missing energy. Also, the $\tilde{\tau}_1$-LSP would decay directly into two jets ($\tilde{\tau}_1 \to \bar{u}d$). We find that this extra lepton from LQD operator will make things worse, although no original missing energy present. Interestingly, the hadronic operator UDD relaxes the LHC constraints due to the missing energy suppression and no extra lepton in the final states. With $\lambda''_{212} \neq 0$, the $\tilde{\chi}_1^0$-LSP decays into three jets ($\tilde{\chi}_1^0 \to cds/\bar{c}\bar{d}\bar{s}$). In this decay mode, the signal to U.L. ratio could be reduced by several times compared to the RPC case. By naively estimation, the $\tilde{\chi}_2^\pm$ mass could be $\sim 50 - 100$ GeV lighter than those in Scenarios I and II. However, when the LSP is light stau or tau-sneutrino rather than neutralino, the rich τ signals from the Higgsino decays and then the LSP light stau or sneutrino decays would give very remarkable

signal significances. And the UDD operator would produce more τs than the LQD operator for the light stau LSP. So the viable Wino mass range gets back to the same level as in Scenarios I and II. Notice that these results are just for heuristic discussions, the systematic analysis is necessary if one is serious about these RPV effects.

By the way, we check the three best-fit points in Table II, and find that they are all excluded as expected from the above discussions.

C. The SUSY Models Consistent with Δa_μ and the LHC SUSY Searches

We will discuss the general results in the SUSY models which are consistent with Δa_μ and the LHC SUSY searches.

1. Generic SUSY Models

Although we consider the EWSUSY in the NMSSM to check the electroweak SUSY sector, the above results can be extended to general SUSY models which can explain Δa_μ. Although the small $\mu_{\rm eff}$ and an extra neutralino from singlino compared to the MSSM would modify the signals to some degree, the features of our results are reliable for more general SUSY models. To keep Δa_μ in the measured range, we need the light Higgsinos, Wino, and muon-sneutrino if the chargino-sneutrino loops give dominant contributions. These light sparticles are constrained by the LHC SUSY searches. Thus, the larger $\tan\beta$ is prefered, which is a general conclusion regardless of any specific SUSY model. If the left-handed sleptons are lighter than Wino, the Wino with mass $\lesssim 450$ GeV are strongly disfavored. Otherwise, the Wino mass is generally not much constrained. We have noticed that a general exploration in the MSSM has been made in Refs. [20, 24]. And our results are in agreement with theirs, although in different SUSY models.

Moreover, when μ is very large resulting in heavy Higgsinos, the Bino-smuon contributions to Δa_μ would dominate by the virtue of large mixing (proportional to $\mu\tan\beta$) between the left-handed and right-handed smuons. Thus, only light Bino and sleptons are relevant sparticles as in Ref. [18]. And the LHC SUSY search bounds can be almost evaded since the Bino production cross section is smaller than Winos and Higgsinos.

2. The Moderate to Large $\tan\beta$ *in the NMSSM*

The NMSSM with small $\tan\beta$ has been studied extensively during the last year, inspired by the SM-like Higgs boson mass about 125 GeV and the possible excess of the Higgs decays to $\gamma\gamma$ channel observed at the LHC. Evidently, the small $\tan\beta$ regime is a salient feature of the NMSSM since the large tree-level contribution to Higgs boson mass can be realized for large λ. However, when we take all the known experimental results into account, the moderate to large $\tan\beta$ in the NMSSM would be more interesting.

In the constrained NMSSM, the large $\tan\beta$ is favored from a global analysis [38] in light of the correct dark matter relic density, XENON100 dark matter search bound, and appropriate contributions to $(g_\mu - 2)/2$, and regardless of which Higgs boson is the one observed at the LHC. However, because λ is very small there, the results are similar to the MSSM. The mixing effects in Higgs sector are negligible as a consequence of such small λ [38].

In this paper, we extend the above conclusion for the favorable larger $\tan\beta \sim \mathcal{O}(10)$ to a more general framework. With the EWSUSY, we have individual soft masses for sleptons, which would relax the tension between Higgs boson mass and Δa_μ even with small $\tan\beta \sim 2$. However, the LHC SUSY search results again prefer the relatively large $\tan\beta$. In relatively large $\tan\beta$ regime, because the tree-level contribution from $\lambda S H_d H_u$ superpotential term to Higgs boson mass is negligible, the only new contribution comes from the mixing effects between the doublet and singlet Higgs fields, with the SM-like Higgs boson being the second lightest one. So the whole contributions to Higgs boson mass are: (1) the tree-level contribution ~ 90 GeV; (2) The radiative corrections from stop quarks ~ 30 GeV; (3) The slight lift from the pushing up effect ~ 5 GeV. The Higgs boson mass features change a little bit in this regime. For relatively large $\tan\beta$, the H_d-like Higgs boson will be heavy at TeV scale (see below for details). If we decouple it for simplicity, the elements of Higgs boson mass matrix can be reduced to

$$M_{hh}^2 \simeq m_Z^2 + \delta m_h^2 \sim 120\text{GeV} \ , \tag{25}$$

$$M_{ss}^2 \simeq \lambda^2 v^2 \frac{A_\lambda}{\mu \tan\beta} + 4\left(\frac{\kappa}{\lambda}\right)^2 \mu^2 + \frac{\kappa}{\lambda} A_\kappa \mu \ , \tag{26}$$

$$M_{sh}^2 \simeq 2\lambda\mu v \left(1 - \frac{A_\lambda}{\mu\tan\beta} - \frac{2\kappa}{\lambda\tan\beta}\right) \ , \tag{27}$$

where δm_h^2 denotes the radiative corrections, and the trilinear soft terms A_λ and A_κ are the values at $M_{\rm SUSY}$. We also use μ instead of $\mu_{\rm eff}$ here for simplicity. For the original

mass matrix, see Refs. [31, 35]. In order to increase the SM-like Higgs boson mass by several GeV, the singlet-like Higgs boson should be the lightest. Thus, the vaccum stability condition ($M_{sh}^4 \leq M_{ss}^2 M_{hh}^2 \lesssim (125\ \text{GeV})^4$) enforces a not so large λ and $A_\lambda \sim \mu \tan\beta \sim \mathcal{O}(150 \times 10)$ GeV. A small μ within several hundred GeV is also needed here to avoid the flipping in the mass order. Because $M_A^2 = \frac{2B_{\rm eff}\mu}{\sin 2\beta} \simeq \mu \tan\beta (A_\lambda + \frac{\kappa}{\lambda}\mu) \sim (\mu \tan\beta)^2$ for relatively large $\tan\beta$, the H_d-like Higgs boson masses are estimated as $\mu \tan\beta$, which is around TeV scale. Therefore, we have two light CP-even neutral Higgs bosons, one light CP-odd Higgs boson, and the other three H_d-like Higgs fields ($H_3, A_2, H^\pm$) are heavy in this relatively large $\tan\beta$ and moderate λ regime. Moreover, the heavy squarks and gluino are needed to provide the desirable radiative corrections to Higgs boson mass.

D. Prospects for the EWSUSY Searches at the LHC-14 and ILC

After the LHC SUSY search constraints have been applied, the survived regions suggest that the EWSUSY might be just above the reach of the current detection capability. The light neutralinos/charginos and sleptons in the EWSUSY are very promising to be observed at the upcoming colliders such as the LHC-14 and ILC. Let us revisit the features of electroweak SUSY sector at first. We have $\tilde{\chi}_1^0$, $\tilde{\chi}_2^0$, and $\tilde{\chi}_3^0$ lighter than ~ 300 GeV, which are mainly the mixtures of $\tilde{H}_u$, $\tilde{H}_d$ and $\tilde{S}$. Also, $\tilde{\chi}_4^0$ and $\tilde{\chi}_5^0$ respectively have dominant Bino and Wino components in most cases. However, when all the neutralinos are within $\sim$300 GeV, there exist the large mixings among them, and no pure mass eigenstates remain. As for charginos, the Higgsino-like $\tilde{\chi}_1^\pm$ are always lighter than about 200 GeV, and $\tilde{\chi}_2^\pm$ is Wino-like. Similar to the neutralino sector, when $\tilde{\chi}_2^\pm$ is also very light, Higgsino and Wino will mix with each other as well. Besides, the light left-handed smuon $\lesssim 500$ GeV are required by Δa_μ, with the other left-handed sleptons and sneutrinos are also light for the sake of $SU(2)_L$ gauge symmetry and family universality. However, the right-handed sleptons are not neccessarily very light since their masses are controled by an independent input parameter $M_{\tilde{E}}$. Their masses range from 100 GeV to 800 GeV in our scan results.

Because a bunch of sparticles may invole in, their mass order is very important for the sparticle decay chains. To be more concrete, we employ some benchmark masses $m_{\tilde{\chi}_2^\pm}$, $m_{\tilde{\chi}_1^\pm}$, $m_{\tilde{\mu}_L}$, and $m_{\tilde{\tau}_1}$ to organize the mass order, where $m_{\tilde{\chi}_2^\pm}$ and $m_{\tilde{\chi}_1^\pm}$ represent Wino and Higgsino masses, respectively. The most typical mass orders are listed as follows: (1) $m_{\tilde{\chi}_2^\pm} >$

$m_{\tilde{\mu}_L} > m_{\tilde{\tau}_1} > m_{\tilde{\chi}_1^\pm}$; (2) $m_{\tilde{\chi}_2^\pm} > m_{\tilde{\mu}_L} > m_{\tilde{\chi}_1^\pm} > m_{\tilde{\tau}_1}$; (3) $m_{\tilde{\mu}_L} > m_{\tilde{\chi}_2^\pm} > m_{\tilde{\tau}_1} > m_{\tilde{\chi}_1^\pm}$; (4) $m_{\tilde{\mu}_L} > m_{\tilde{\chi}_2^\pm} > m_{\tilde{\chi}_1^\pm} > m_{\tilde{\tau}_1}$. In these orders, the first two terms influence the Wino-like $\tilde{\chi}_2^\pm$ and $\tilde{\chi}_5^0$ decays, while the last two terms control the decays of the Higgsino-like $\tilde{\chi}_1^\pm$ and $\tilde{\chi}_{2/3}^0$. As for these sparticle productions, the cross sections for the neutralino-chargino and chargino-chargino pair productions are the largest at the LHC. In the following, we will discuss the procuction processes separately:

- Higgsinos: Higgsinos are very light and then have large production cross sections. They tend to decay into light stau and/or tau-snertrino if kinematically allowed, as in mass orders (2) and (4). So the rich τ signatures are noticable in this case. If light stau and tau-sneutrino are heavy as in mass orders (1) and (3), the Higgsino decays will mediated by virtual gauge bosons in most cases. Unfortunately, the small mass difference between the produced Higgsinos and LSP blocks the visible final states, resulting in little observable signals. In general, we have $\Delta m \equiv m_{\tilde{\chi}_i^{0/\pm}} - m_{\tilde{\chi}_1^0} \sim 10 - 100$ GeV. Ref. [51] discussed the signature of soft di-leptons at the LHC. Perhaps similar techniques could be applied to the Higgsino searches together with the Vector Boson Fusion (VBF) production processes which could reduce the backgrounds drastically [52]. Actually, Higgsinos will serve as the more important roles in the cascade decays of Bino and Winos than in direct production.

- Bino and Winos: Main production processes would be Wino pair productions. Bino has small production cross section, and mainly manifest itself in Wino decays. With Higgsinos lighter than them, they will experience longer cascade decay chains. The Bino and Wino decays are highly dependent on the left-handed slepton mass. In mass orders (1) and (2), the left-handed sleptons are lighter and will take control of the decay chains, resulting in the golden tri-lepton signature in $\tilde{\chi}^\pm\tilde{\chi}^0$ pair-productions. Especially, in mass order (2), up to 7 leptons would emerge if Higgsinos all decay into τs. We list this long cascade decay chain here: $pp \to \tilde{\chi}_2^\pm\tilde{\chi}_5^0 \to (\tilde{l}\nu)(\tilde{l}l) \to (\tilde{\chi}_4^0 l^\pm\nu)(\tilde{\chi}_4^0 l^\pm l^\mp)$. With Bino-like $\tilde{\chi}_4^0$ mainly decaying into $\tilde{\tau}_1\tau$ ($\tilde{\tau}_1$ is almost right-handed.), such decay chain ends in $(\tau^+\tau^- l^\pm\nu\tilde{\chi}_1^0)(\tau^+\tau^- l^+ l^-\tilde{\chi}_1^0)$. Ref. [53] has discussed the many-lepton signatures from very long cascade decay chains in the NMSSM, although its particle content is a little bit different from here. On the other hand, in mass orders (3) and (4) with $m_{\tilde{\mu}_L} > m_{\tilde{\chi}_2^\pm}$ (From the subsection IV B, Winos could be very light in these

cases and then have very large production cross sections.), Winos will generically decay into several gauge bosons on-shell or off-shell, depending on the mass splittings and specific mass order. Taking the decay chain $pp \to \tilde{\chi}_2^{\pm}\tilde{\chi}_5^0 \to (\tilde{\chi}_1^{\pm}Z)(\tilde{\chi}_1^{\pm}W^{\mp})$ as an example, it would end either in $(W^{\pm(*)}Z\tilde{\chi}_1^0)(W^{\pm(*)}W^{\mp}\tilde{\chi}_1^0)$ for mass order (4) or in $(\tilde{\tau}_1\nu_\tau Z)(\tilde{\tau}_1\nu_\tau W^{\mp}) \to (\tau\nu_\tau Z\tilde{\chi}_1^0)(\tau^{\pm}\nu_\tau W^{\pm}\tilde{\chi}_1^0)$ for mass order (3). Thus, the leptons (τ is very important in some cases) and gauge bosons in final states are typical signatures. In addition to slepton and gauge boson decay modes, there would be several percent branching fraction into Higgs final states such as $\tilde{\chi}_2^{\pm} \to \tilde{\chi}_1^{\pm}(H/A)$ and $\tilde{\chi}_5^0 \to \tilde{\chi}_{1/2/3}^0(H/A)$. The Higgs decay modes have been considered in Refs. [54, 55], which explored the WH final states. As the concrete examples for different decay patterns discussed above, one can refer to the benchmark points in Tables III and IV.

- Sleptons: When Winos are too heavy to explore, sleptons must be light enough to accomodate with Δa_μ. Thus, we could focus on the slepton pair productions instead. Light sleptons have large production cross sections at the ILC, and the opposite-sign di-leptons are typical signatures.

In short, the very interesting patterns would emerge in the searches for electroweak SUSY sector, which definitely deserve further deep study. We just present several naive ideas here, and leave the dedicated analyses for a future work.

V. CONCLUSION

Taking into account all the available experimental constraints/results, especially the 125 GeV SM-like Higgs boson at the LHC and the muon anomalous magnetic moment, we have studied the EWSUSY in details in the NMSSM for three scenarios. Using χ^2 statistic test, we obtained the most favorable regions in the whole parameter space. Moreover, we found that the LHC SUSY searches for neutralinos/charginos and sleptons have already put considerable constraints on the electroweak SUSY sector. And then the favored model parameter space and the resulting mass spectra are modified accordingly. After the systematic analyses, we are led to the following conclusions:

- Unlike the previous studies in the NMSSM, we found that the moderdate to large $\tan\beta \sim \mathcal{O}(10)$ is prefered after the LHC SUSY search bounds are taken into account.

The relatively large $\tan\beta$ can be compatible with the muon anomalous magnetic moment and SM-like Higgs boson mass simultaneously. Especially, the SM-like Higgs boson is the second lightest CP-even neutral Higgs boson, whose mass is lifted a little bit further by pushing up effect.

- The squarks and gluino are heavy around a few TeV and is out of the current LHC reach. The light electroweak SUSY sector lies on the brim of the current detection capability. In particular, the EWSUSY in the NMSSM can fit into all the current experimental data very well with $\chi^2/\text{DOF} \sim 1$. All the charginos, neutralinos, and sleptons are around several hundred GeV.

- The current LHC SUSY searches have put strong constraints on the light electroweak SUSY sector through the lepton final states. And the sparticle masses related to Δa_μ are constrained by these results as displayed in Figs. 6 and 7. Generically speaking, a Wino-like $\tilde{\chi}_2^\pm$ lighter than ~ 450 GeV may be excluded when the left-handed sleptons are lighter than it. However, with the left-handed sleptons heavier or nearly mass-degenerate with it, no definite constraint on the $\tilde{\chi}_2^\pm$ mass could be obtained. And a light $\tilde{\chi}_2^\pm$ with mass around 230 GeV is still viable.

- The searches for electroweak SUSY sector of the EWSUSY in the NMSSM is promising at the LHC-14 and ILC, and definitely deserve further dedicated analyses. The lepton final states are very important, and the promising signatures include the multi-leptons (The number of leptons can be up to 7.), τ leptons, oppsite-sign di-leptons, and so on. In addition, the searches for Higgs bosons as final states would be very promising if Winos are very light and then have large production cross sections.

Acknowledgments

This research was supported in part by the Natural Science Foundation of China under grant numbers 10821504, 11075194, 11135003, 11275246, and by the DOE grant DE-FG03-

95-Er-40917 (TL).

---

[1] A. Djouadi, Phys. Rept. **459**, 1 (2008) [hep-ph/0503173].

[2] G. Aad *et al.* [ATLAS Collaboration], Phys. Lett. B **716**, 1 (2012) [arXiv:1207.7214 [hep-ex]].

[3] S. Chatrchyan *et al.* [CMS Collaboration], Phys. Lett. B **716**, 30 (2012) [arXiv:1207.7235 [hep-ex]].

[4] https://twiki.cern.ch/twiki/bin/view/AtlasPublic/HiggsPublicResults; https://twiki.cern.ch/twiki/bin/view/CMSPublic/PhysicsResultsHIG.

[5] https://twiki.cern.ch/twiki/bin/view/AtlasPublic/SupersymmetryPublicResults; https://twiki.cern.ch/twiki/bin/view/CMSPublic/PhysicsResultsSUS.

[6] RAaij *et al.* [LHCb Collaboration], Phys. Rev. Lett. **110**, 021801 (2013) [arXiv:1211.2674 [Unknown]].

[7] O. Buchmueller, R. Cavanaugh, A. De Roeck, J. R. Ellis, H. Flacher, S. Heinemeyer, G. Isidori and K. A. Olive *et al.*, Eur. Phys. J. C **64**, 391 (2009) [arXiv:0907.5568 [hep-ph]].

[8] E. Barberio *et al.* [Heavy Flavor Averaging Group (HFAG) Collaboration], arXiv:0704.3575 [hep-ex].

[9] D. Asner *et al.* [Heavy Flavor Averaging Group Collaboration], arXiv:1010.1589 [hep-ex].

[10] Y. Amhis *et al.* [Heavy Flavor Averaging Group Collaboration], arXiv:1207.1158 [hep-ex].

[11] M. Davier, A. Hoecker, B. Malaescu and Z. Zhang, Eur. Phys. J. C **71**, 1515 (2011) [Erratum-ibid. C **72**, 1874 (2012)] [arXiv:1010.4180 [hep-ph]].

[12] G. Hinshaw *et al.* [WMAP Collaboration], arXiv:1212.5226 [astro-ph.CO].

[13] E. Aprile *et al.* [XENON100 Collaboration], Phys. Rev. Lett. **109**, 181301 (2012) [arXiv:1207.5988 [astro-ph.CO]].

[14] T. Cheng, J. Li, T. Li, D. V. Nanopoulos and C. Tong, Eur. Phys. J. C **73**, 2322 (2013) [arXiv:1202.6088 [hep-ph]].

[15] T. Li and D. V. Nanopoulos, Phys. Lett. B **692**, 121 (2010) [arXiv:1002.4183 [hep-ph]].

[16] C. Balazs, T. Li, D. V. Nanopoulos and F. Wang, JHEP **1009**, 003 (2010) [arXiv:1006.5559 [hep-ph]].

[17] G. F. Giudice, P. Paradisi, A. Strumia and A. Strumia, JHEP **1210**, 186 (2012) [arXiv:1207.6393 [hep-ph]].

[18] M. Ibe, S. Matsumoto, T. T. Yanagida and N. Yokozaki, JHEP **1303**, 078 (2013) [arXiv:1210.3122 [hep-ph]].

[19] P. Grajek, A. Mariotti and D. Redigolo, arXiv:1303.0870 [hep-ph].

[20] M. Endo, K. Hamaguchi, S. Iwamoto and T. Yoshinaga, arXiv:1303.4256 [hep-ph].

[21] S. Mohanty, S. Rao and D. P. Roy, arXiv:1303.5830 [hep-ph].

[22] G. Bhattacharyya, B. Bhattacherjee, T. T. Yanagida and N. Yokozaki, arXiv:1304.2508 [hep-ph].

[23] S. Akula and P. Nath, arXiv:1304.5526 [hep-ph].

[24] S. Iwamoto, arXiv:1304.5171 [hep-ph].

[25] A. Choudhury and A. Datta, arXiv:1305.0928 [hep-ph].

[26] T. Moroi, Phys. Rev. D **53**, 6565 (1996) [Erratum-ibid. D **56**, 4424 (1997)] [hep-ph/9512396].

[27] S. P. Martin and J. D. Wells, Phys. Rev. D **64**, 035003 (2001) [hep-ph/0103067].

[28] M. Byrne, C. Kolda and J. E. Lennon, Phys. Rev. D **67**, 075004 (2003) [hep-ph/0208067].

[29] D. Stockinger, J. Phys. G **34**, R45 (2007) [hep-ph/0609168].

[30] F. Domingo and U. Ellwanger, JHEP **0807**, 079 (2008) [arXiv:0806.0733 [hep-ph]].

[31] U. Ellwanger, C. Hugonie and A. M. Teixeira, Phys. Rept. **496**, 1 (2010) [arXiv:0910.1785 [hep-ph]].

[32] U. Ellwanger, JHEP **1203**, 044 (2012) [arXiv:1112.3548 [hep-ph]].

[33] J. F. Gunion, Y. Jiang and S. Kraml, Phys. Lett. B **710**, 454 (2012) [arXiv:1201.0982 [hep-ph]].

[34] S. F. King, M. Muhlleitner and R. Nevzorov, Nucl. Phys. B **860**, 207 (2012) [arXiv:1201.2671 [hep-ph]].

[35] Z. Kang, J. Li and T. Li, JHEP **1211**, 024 (2012) [arXiv:1201.5305 [hep-ph]].

[36] U. Ellwanger and C. Hugonie, Adv. High Energy Phys. **2012**, 625389 (2012) [arXiv:1203.5048 [hep-ph]].

[37] J. F. Gunion, Y. Jiang and S. Kraml, Phys. Rev. D **86**, 071702 (2012) [arXiv:1207.1545 [hep-ph]].

[38] K. Kowalska, S. Munir, L. Roszkowski, E. M. Sessolo, S. Trojanowski and Y. -L. S. Tsai, arXiv:1211.1693 [hep-ph].

[39] L. J. Hall, D. Pinner and J. T. Ruderman, JHEP **1204**, 131 (2012) [arXiv:1112.2703 [hep-ph]]; J. -J. Cao, Z. -X. Heng, J. M. Yang, Y. -M. Zhang and J. -Y. Zhu, JHEP **1203**, 086 (2012) [arXiv:1202.5821 [hep-ph]]; D. A. Vasquez, G. Belanger, C. Boehm, J. Da Silva, P. Richard-

son and C. Wymant, Phys. Rev. D **86**, 035023 (2012) [arXiv:1203.3446 [hep-ph]]; T. Graf, R. Grober, M. Muhlleitner, H. Rzehak and K. Walz, JHEP **1210**, 122 (2012) [arXiv:1206.6806 [hep-ph]]; R. Benbrik, M. Gomez Bock, S. Heinemeyer, O. Stal, G. Weiglein and L. Zeune, Eur. Phys. J. C **72**, 2171 (2012) [arXiv:1207.1096 [hep-ph]]; B. Kyae and J. -C. Park, arXiv:1207.3126 [hep-ph]; J. Cao, Z. Heng, J. M. Yang and J. Zhu, JHEP **1210**, 079 (2012) [arXiv:1207.3698 [hep-ph]]; T. Cheng, J. Li, T. Li, X. Wan, Y. k. Wang and S. -h. Zhu, arXiv:1207.6392 [hep-ph]; M. Perelstein and B. Shakya, arXiv:1208.0833 [hep-ph]; J. F. Gunion, Y. Jiang and S. Kraml, Phys. Rev. Lett. **110**, 051801 (2013) [arXiv:1208.1817 [hep-ph]]; K. J. Bae, K. Choi, E. J. Chun, S. H. Im, C. B. Park and C. S. Shin, JHEP **1211**, 118 (2012) [arXiv:1208.2555 [hep-ph]]; Z. Kang, T. Li, J. Li and Y. Liu, arXiv:1208.2673 [hep-ph]; G. Belanger, U. Ellwanger, J. F. Gunion, Y. Jiang and S. Kraml, arXiv:1208.4952 [hep-ph]; K. Agashe, Y. Cui and R. Franceschini, JHEP **1302**, 031 (2013) [arXiv:1209.2115 [hep-ph]]; I. Gogoladze, B. He and Q. Shafi, Phys. Lett. B **718**, 1008 (2013) [arXiv:1209.5984 [hep-ph]]; G. Belanger, U. Ellwanger, J. F. Gunion, Y. Jiang, S. Kraml and J. H. Schwarz, JHEP **1301**, 069 (2013) [arXiv:1210.1976 [hep-ph]]; K. Choi, S. H. Im, K. S. Jeong and M. Yamaguchi, JHEP **1302**, 090 (2013) [arXiv:1211.0875 [hep-ph]]; K. Schmidt-Hoberg, F. Staub and M. W. Winkler, JHEP **1301**, 124 (2013) [arXiv:1211.2835 [hep-ph]]; S. F. King, M. Mhlleitner, R. Nevzorov and K. Walz, Nucl. Phys. B **870**, 323 (2013) [arXiv:1211.5074 [hep-ph]]; T. Gherghetta, B. von Harling, A. D. Medina and M. A. Schmidt, JHEP **1302**, 032 (2013) [arXiv:1212.5243 [hep-ph]]; Z. Kang, J. Li, T. Li, D. Liu and J. Shu, arXiv:1301.0453 [hep-ph]; D. Das, U. Ellwanger and A. M. Teixeira, JHEP **1304**, 117 (2013) [arXiv:1301.7584 [hep-ph]]; N. D. Christensen, T. Han, Z. Liu and S. Su, arXiv:1303.2113 [hep-ph]; T. Cheng, J. Li, T. Li and Q. -S. Yan, arXiv:1304.3182 [hep-ph]; S. Moretti, S. Munir and P. Poulose, arXiv:1305.0166 [hep-ph]; S. Munir, L. Roszkowski and S. Trojanowski, arXiv:1305.0591 [hep-ph]; G. D. Kribs, A. Martin and A. Menon, arXiv:1305.1313 [hep-ph].

[40] M. Badziak, M. Olechowski and S. Pokorski, arXiv:1304.5437 [hep-ph].

[41] B. C. Allanach, M. A. Bernhardt, H. K. Dreiner, C. H. Kom and P. Richardson, Phys. Rev. D **75**, 035002 (2007) [hep-ph/0609263].

[42] LEP2 SUSY Working Group, http://lepsusy.web.cern.ch/lepsusy/www/rpvllesummer02/lle_pub.html.

[43] U. Ellwanger, J. F. Gunion and C. Hugonie, JHEP **0502**, 066 (2005) [hep-ph/0406215].

[44] G. Belanger, F. Boudjema, A. Pukhov and A. Semenov, Comput. Phys. Commun. **174**, 577 (2006) [hep-ph/0405253].

[45] S. Chatrchyan *et al.* [CMS Collaboration], arXiv:1209.6620 [hep-ex]; G. Aad *et al.* [ATLAS Collaboration], arXiv:1208.2884 [hep-ex]; G. Aad *et al.* [ATLAS Collaboration], arXiv:1208.3144 [hep-ex]; CMS Collaboration, CMS-PAS-SUS-12-022; ATLAS Collaboration, ATLAS-CONF-2012-154; ATLAS Collaboration, ATLAS-CONF-2013-035.

[46] J. Alwall, M. Herquet, F. Maltoni, O. Mattelaer and T. Stelzer, JHEP **1106**, 128 (2011) [arXiv:1106.0522 [hep-ph]].

[47] T. Sjostrand, S. Mrenna and P. Z. Skands, JHEP **0605**, 026 (2006) [hep-ph/0603175].

[48] J. Conway, PGS4, URL http://physics.ucdavis.edu/∼conway/research/software/pgs/pgs4-general.htm.

[49] S. Y. Choi, D. J. Miller, and P. M. Zerwas, Nucl. Phys. B **711**, 83 (2005) [hep-ph/0407209]; Beenakker, W. and Klasen, M. and Krämer, M. and Plehn, T. and Spira, M. and Zerwas, P. M. Phys. Rev. Lett. **3780**, 83 (1999).

[50] S. Ovyn, X. Rouby and V. Lemaitre, arXiv:0903.2225 [hep-ph].

[51] S. Kraml, A. R. Raklev and M. J. White, Phys. Lett. B **672**, 361 (2009) [arXiv:0811.0011 [hep-ph]].

[52] B. Dutta, A. Gurrola, W. Johns, T. Kamon, P. Sheldon and K. Sinha, arXiv:1210.0964 [hep-ph].

[53] V. Barger, G. Shaughnessy and B. Yencho, Phys. Rev. D **83**, 055006 (2011) [arXiv:1011.3526 [hep-ph]].

[54] H. Baer, V. Barger, A. Lessa and X. Tata, Phys. Rev. D **86**, 117701 (2012) [arXiv:1207.4846 [hep-ph]].

[55] D. Ghosh, M. Guchait and D. Sengupta, Eur. Phys. J. C **72**, 2141 (2012) [arXiv:1202.4937 [hep-ph]].

χ^2_{min} Points:	I	II	III
Param. at $M_{\rm GUT}$:(GeV)			
M_0	1758	1576	1580
M_L	7.1	21	47
M_E	304	251	272
M_1	348	256	343
M_2	209	202	182
M_3	556	336	585
A_0	-1955	-2354	-2480
A_E	-7964	-4801	-5569
A_λ	-618	-854	-751
A_κ	-0.02	-0.01	-0.02
Param. at $M_{\rm SUSY}$:			
λ	0.615	0.650	0.582
κ	0.082	0.134	0.085
$\tan\beta$	1.94	1.98	1.97
$\mu_{\rm eff}$	204	189	254
Spectrum:(GeV)			
H_1	88	111	99
H_2	**125.2**	**125.4**	**124.8**
H_3	490	448	616
A_1	108	85	111
A_2	494	450	618
$H^\pm$	482	437	610
$\tilde{\chi}^0_1$	65	62	77
$\tilde{\chi}^0_2$	117	115	120
$\tilde{\chi}^0_3$	152	140	145
$\tilde{\chi}^0_4$	-242	-228	-282
$\tilde{\chi}^0_5$	277	266	306
$\tilde{\chi}^\pm_1$	111	104	110
$\tilde{\chi}^\pm_2$	268	258	296
$\tilde{g}$	1360	873	1413

χ^2_{min} Points:	I	II	III
$\tilde{\nu}_{e/\mu}$	158	127	181
$\tilde{\nu}_\tau$	125	112	167
$\tilde{e}_R/\tilde{\mu}_R$	221	197	133
$\tilde{e}_L/\tilde{\mu}_L$	168	140	190
$\tilde{\tau}_1$	93	108	64
$\tilde{\tau}_2$	203	190	190
$\tilde{t}_1$	859	472	750
$\tilde{t}_2$	1051	704	1021
$\tilde{b}_1$	996	632	970
$\tilde{b}_2$	2479	2119	2298
$\tilde{u}_R/\tilde{c}_R$	2497	2129	2325
$\tilde{u}_L/\tilde{c}_L$	1916	1571	1821
$\tilde{d}_R/\tilde{s}_R$	2497	2133	2322
$\tilde{d}_L/\tilde{s}_L$	1916	1572	1822
Pheno.			
$R_{\gamma\gamma}$	1.32	1.28	1.36
R_{VV}	1.02	1.02	0.97
R_{Vbb}	0.90	0.80	0.82
$R_{\tau\tau}$	0.94	0.85	0.85
$\mathrm{BR}(b\to s\gamma)/10^{-4}$	3.77	3.54	3.54
$\mathrm{BR}(b\to \tau\nu)/10^{-4}$	1.32	1.32	1.32
$\mathrm{BR}(B_s\to \mu^+\mu^-)/10^{-9}$	3.67	3.67	3.67
$\Delta a_\mu/10^{-9}$	2.64	2.85	2.74
Ωh^2	0.1157	7×10^{-5}	–
$\sigma_p^{SI}/10^{-9}pb$	1.6	46	–

TABLE II: The best χ^2 fit points for three scenarios: χ^2_{min}/DOF=10.2/15, χ^2_{min}/DOF=9.6/14, and χ^2_{min}/DOF=9.2/14 for Scenarios I, II, and III, respectively.

Points:	I	II	III
Param. at $M_{\rm GUT}$:(GeV)			
M_0	2267	1746	2006
M_L	650	572	766
M_E	550	199	210
M_1	-348	-504	-360
M_2	376	442	353
M_3	-1435	-1924	-1429
A_0	60	121	121
A_E	-209	-573	-612
A_λ	4352	4625	4575
A_κ	836	421	418
Param. at $M_{\rm SUSY}$:			
λ	0.296	0.208	0.207
κ	0.103	0.084	0.08
$\tan\beta$	16	19.8	19.2
$\mu_{\rm eff}$	162	129	143
Spectrum:(GeV)			
H_1	98	90	94
H_2	125.3	125	125
H_3	2883	2978	3151
A_1	82	68	73
A_2	2883	2978	3151
$H^\pm$	2883	2979	3152
$\tilde{\chi}_1^0$	100	92	99
$\tilde{\chi}_2^0$	-127	-131	-123
$\tilde{\chi}_3^0$	175	143	150
$\tilde{\chi}_4^0$	-193	-217	-181
$\tilde{\chi}_5^0$	378	439	359
$\tilde{\chi}_1^\pm$	155	127	136
$\tilde{\chi}_2^\pm$	379	439	359
$\tilde{g}$	-3212	-4132	-3179
$\tilde{t}_1$	2763	3146	2646
$\tilde{q}_{\rm min}$	3345	3810	3203

Points:	I	II	III
$\tilde{\nu}_{e/\mu}$	339	362	435
$\tilde{\nu}_\tau$	200	108	249
$\tilde{e}_R/\tilde{\mu}_R$	961	724	921
$\tilde{e}_L/\tilde{\mu}_L$	348	370	442
$\tilde{\tau}_1$	214	132	261
$\tilde{\tau}_2$	879	532	770
Pheno.			
$R_{\gamma\gamma}$	1.1	1.04	1.0
R_{VV}	0.99	1	0.96
R_{Vbb}	0.66	0.76	0.73
$R_{\tau\tau}$	0.67	0.77	0.74
BR$(B\to X_s\gamma)/10^{-4}$	3.22	3.22	3.21
BR$(B\to\tau\nu_\tau)/10^{-4}$	1.32	1.31	1.32
BR$(B_s^0\to\mu^+\mu^-)/10^{-9}$	3.68	3.68	3.68
$\Delta a_\mu/10^{-9}$	2.15	2.32	2.1
Ωh^2	0.11	0.103	0.1
$\sigma_p^{SI}/10^{-9}pb$	2.2	1.3	2.8
BRs of Dominant Decay Modes			
$\tilde{\chi}_2^\pm\to\tilde{l}_L\nu/\tilde{\nu}l$	0.34	0.51	0.22
$\tilde{\chi}_2^\pm\to\tilde{\chi}_1^\pm Z$	0.16	0.12	0.20
$\tilde{\chi}_2^\pm\to\tilde{\chi}_1^0 W^\pm$	0.07	0.06	0.09
$\tilde{\chi}_2^\pm\to\tilde{\chi}_2^0 W^\pm$	0.05	0.11	0.11
$\tilde{\chi}_2^\pm\to\tilde{\chi}_3^0 W^\pm$	0.11	0.07	0.13
$\tilde{\chi}_2^\pm\to\tilde{\chi}_1^\pm H_2$	0.06	0.08	0.09
$\tilde{\chi}_5^0\to\tilde{l}_L l/\tilde{\nu}\nu$	0.35	0.52	0.22
$\tilde{\chi}_5^0\to\tilde{\chi}_1^\pm W^\mp$	0.35	0.26	0.46
$\tilde{\chi}_5^0\to\tilde{\chi}_2^0 Z$	0.04	0.08	0.08
$\tilde{\chi}_2^\pm\to\tilde{\chi}_1^0 H_2$	0.02	0.02	0.03
$\tilde{e}_L/\tilde{\mu}_L\to\tilde{\chi}_1^\pm\nu$	0.12	0.07	0.07
$\tilde{e}_L/\tilde{\mu}_L\to\tilde{\chi}_1^0 e/\mu$	0.09	0.1	0.05
$\tilde{e}_L/\tilde{\mu}_L\to\tilde{\chi}_2^0 e/\mu$	0.61	0.27	0.28
$\tilde{\tau}_1\to\tilde{\chi}_1^\pm\tau$	0.08	–	0.09
$\tilde{\tau}_1\to\tilde{\chi}_1^0\tau$	0.15	0.99	0.13
$\tilde{\tau}_1\to\tilde{\chi}_2^0\tau$	0.68	–	0.51

TABLE III: The benchmark points satisfy the LHC SUSY search constraints in Scenario I. Here, $\tilde{q}_{\rm min}$ denotes the lightest squark in the first two generations. The kinematically forbidden or negligible decay modes are presented in dashes.

Points:	I	II	III	IV
Param. at $M_{\rm GUT}$:(GeV)				
M_0	903	2699	390	1639
M_L	28	12	24	30
M_E	558	0.6	567	270
M_1	-313	680	-517	340
M_2	278	762	163	221
M_3	-1199	558	-1536	520
A_0	3453	-3865	1818	-2873
A_E	-109	1.1	-80	-2523
A_λ	4115	-0.7	3862	-545
A_κ	224	-84	315	-0.01
Param. at $M_{\rm SUSY}$:				
λ	0.19	0.34	0.31	0.613
κ	0.08	0.26	0.26	0.123
$\tan\beta$	12.1	9.4	11.5	2.48
$\mu_{\rm eff}$	148	111	168	268
Spectrum:(GeV)				
H_1	107	94	95	69
H_2	125.4	124.8	126.0	124.7
H_3	1996	1133	2085	752
A_1	116	242	439	213
A_2	1996	1132	2084	753
$H^\pm$	1997	1133	2085	745
$\tilde{\chi}_1^0$	107	87	112	97
$\tilde{\chi}_2^0$	-114	-126	-167	142
$\tilde{\chi}_3^0$	150	199	-229	164
$\tilde{\chi}_4^0$	-177	298	232	-296
$\tilde{\chi}_5^0$	293	643	297	324
$\tilde{\chi}_1^\pm$	130	110	119	142
$\tilde{\chi}_2^\pm$	293	643	242	313
$\tilde{g}$	-2642	1421	-3298	1277
$\tilde{t}_1$	1085	1641	1966	718
$\tilde{q}_{\rm min}$	2403	2683	2850	1792

Points:	I	II	III	IV
$\tilde{\nu}_{e/\mu}$	323	160	318	138
$\tilde{\nu}_\tau$	293	145	287	132
$\tilde{e}_R/\tilde{\mu}_R$	374	622	378	221
$\tilde{e}_L/\tilde{\mu}_L$	332	178	327	153
$\tilde{\tau}_1$	301	164	296	143
$\tilde{\tau}_2$	322	615	326	217
Pheno.				
$R_{\gamma\gamma}$	1.02	1.29	1.11	1.11
R_{VV}	0.97	1.18	1.02	1.02
R_{Vbb}	0.8	0.67	0.71	0.96
$R_{\tau\tau}$	0.8	0.68	0.72	0.96
BR$(B\to X_s\gamma)/10^{-4}$	3.46	3.28	3.29	3.33
BR$(B\to\tau\nu_\tau)/10^{-4}$	1.32	1.31	1.32	1.32
BR$(B_s^0\to\mu^+\mu^-)/10^{-9}$	3.68	3.66	3.68	3.67
$\Delta a_\mu/10^{-9}$	2.15	1.78	2.41	1.63
Ωh^2	0.02	0.03	0.002	0.02
$\sigma_p^{SI}/10^{-9}pb$	11	0.9	39	11
BRs of Dominant Decay Modes				
$\tilde{\chi}_2^\pm\to\tilde{l}_L\nu/\tilde{\nu}l$	–	0.72	–	0.35
$\tilde{\chi}_2^\pm\to\tilde{\chi}_1^\pm Z$	0.28	0.07	0.33	0.18
$\tilde{\chi}_2^\pm\to\tilde{\chi}_1^0 W^\pm$	0.20	0.06	0.57	0.07
$\tilde{\chi}_2^\pm\to\tilde{\chi}_2^0 W^\pm$	0.14	0.07	–	0.04
$\tilde{\chi}_2^\pm\to\tilde{\chi}_3^0 W^\pm$	0.14	–	–	0.22
$\tilde{\chi}_2^\pm\to\tilde{\chi}_1^\pm H_2$	0.08	0.05	0.10	0.06
$\tilde{\chi}_5^0\to\tilde{l}_L l/\tilde{\nu}\nu$	–	0.72	–	0.35
$\tilde{\chi}_5^0\to\tilde{\chi}_1^\pm W^\mp$	0.70	0.15	0.48	0.36
$\tilde{\chi}_5^0\to\tilde{\chi}_2^0 Z$	0.10	0.05	0.26	0.05
$\tilde{\chi}_2^\pm\to\tilde{\chi}_1^0 H_2$	0.03	0.03	0.11	0.09
$\tilde{e}_L/\tilde{\mu}_L\to\tilde{\chi}_1^\pm\nu$	0.19	0.82	0.37	0.63
$\tilde{e}_L/\tilde{\mu}_L\to\tilde{\chi}_1^0 e/\mu$	0.13	0.10	0.26	0.28
$\tilde{e}_L/\tilde{\mu}_L\to\tilde{\chi}_2^0 e/\mu$	0.34	0.09	0.07	0.09
$\tilde{\tau}_1\to\tilde{\chi}_1^\pm\tau$	0.24	0.12	0.43	0.02
$\tilde{\tau}_1\to\tilde{\chi}_1^0\tau$	0.15	0.63	0.31	0.98
$\tilde{\tau}_1\to\tilde{\chi}_2^0\tau$	0.44	0.25	0.08	–

TABLE IV: The benchmark points satisfy the LHC SUSY search constraints in Scenario II. Here, $\tilde{q}_{\rm min}$ denotes the lightest squark in the first two generations. The kinematically forbidden or negligible decay modes are presented in dashes.